

Different Techniques for (and Some Success In) Measurement of Bs

B.V. Jackson

H.-S. Yu, P.P. Hick, A. Buffington,
*Center for Astrophysics and Space Sciences,
University of California at San Diego, LaJolla, CA, USA*

M. Tokumaru, Ken'ichi Fujiki

*Institute for Space-Earth Environmental Research (ISEE),
Nagoya University, Furo-cho, Chikusa-ku, Nagoya 464-8601, Japan*

D. Odstrcil

*George Mason University, 4400 University Drive, Fairfax, VA 22030, USA and
NASA/GSFC M/C 674, Greenbelt, MD 20771, USA*

M.M. Bisi

*RAL Space, STFC Rutherford Appleton Laboratory,
Harwell Campus, Oxfordshire, UK*

J. Kim, J Yun

*Korean Space Weather Center, National Radio Research Agency, 198-6,
Gwideok-ro, Hallim-eup, Jeju-si, Jeju-do, 695-922 South Korea*

<http://ips.ucsd.edu/>

<http://smei.ucsd.edu/>

Different Techniques for Measurement of B_z

Introduction:

B_z : Definition

Geocentric Solar

Magnetospheric (GSM) B_z :

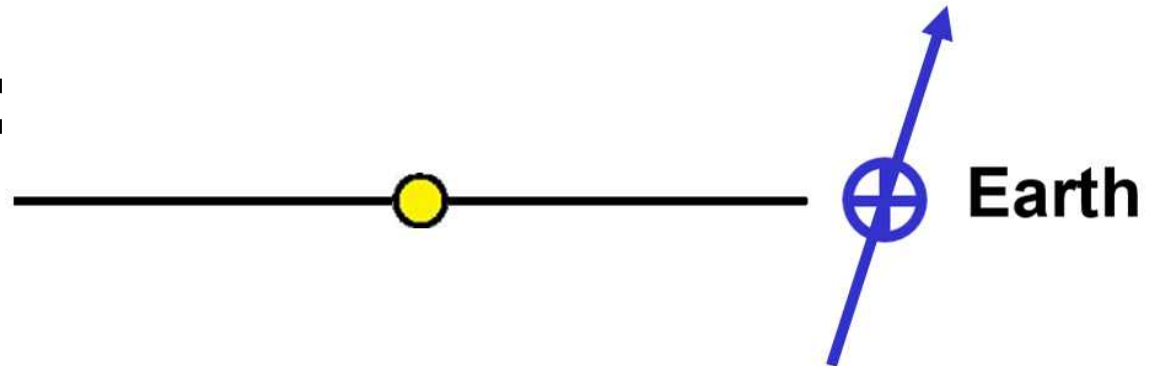
The reasons to determine B_z

Concept studies: How we may be able to determine B_z

1) In CMEs.

2) In the background solar wind

Some successes in determining B_z



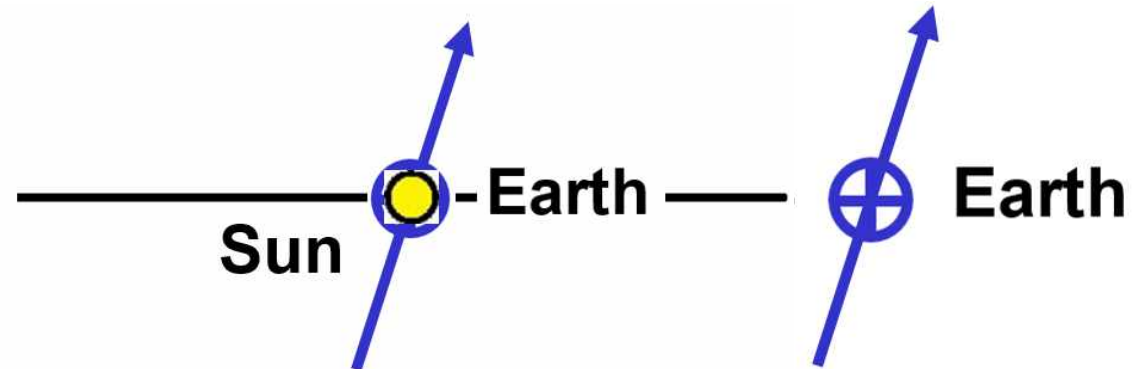
Different Techniques for Measurement of Bz

Introduction:

Bs: Definition

Geocentric Solar

Magnetospheric (GSM) Bz:



The reasons to determine Bz

Concept studies: How we may be able to determine Bz

- 1) In CMEs.**
- 2) In the background solar wind**

Some successes in determining Bz

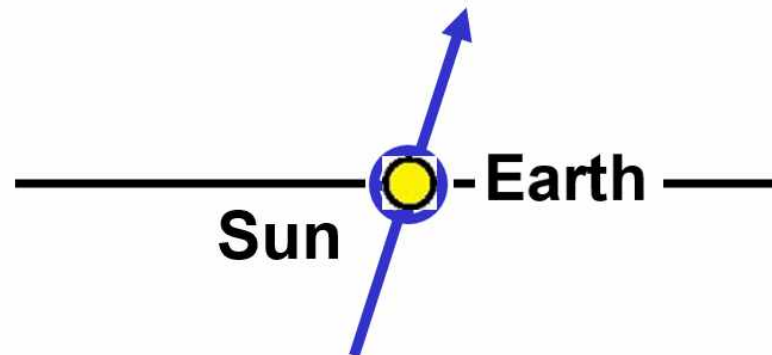
Different Techniques for Measurement of Bz

Introduction:

Bs: Definition

Geocentric Solar

Magnetospheric (GSM) Bz:



The reasons to determine Bz

Concept studies: How we may be able to determine Bz

- 1) In CMEs.**
- 2) In the background solar wind**

Some successes in determining Bz

Different Techniques for Measurement of Bz

Why Determine Bz?

Geomagnetic Substorm Activity

A brief (2-3 hour) disturbance in Earth's magnetosphere that releases energy from the tail of the magnetosphere causing particles to be injected into the high latitude ionosphere.

Geomagnetic Storm Activity

A series of substorms, or a strong or prolonged enhancement of the global magnetospheric electric field.

Both cause radio communication difficulties, particle precipitation into the ionosphere, aurora, satellite damage, ground-based currents, etc.,

A southward IMF is a common factor in the occurrence of both storms and substorms.

Different Techniques for Measurement of Bz

Generally the largest storms and substorms are associated with CMEs

Two factors in CMEs are important.

1) Southward Bz.

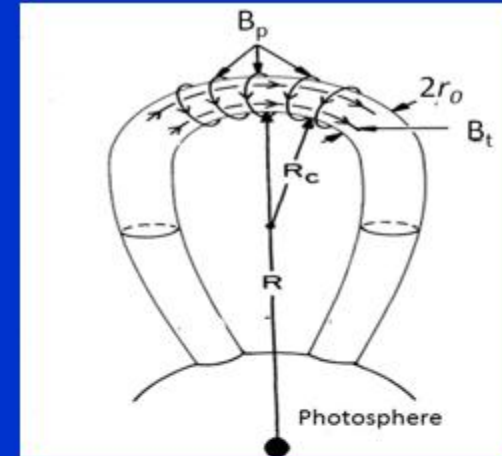
2) Dynamic pressure caused by high speed wind.

Different Techniques for Measurement of B_z CMEs

Fm N. Gopalswamy

Motivation

- All CMEs reaching 1-AU seem to have flux rope structure (irrespective of observed MC or non-MC structure of ICMEs)



Mouschovias and Poland, 1978

Both geometrical and magnetic properties of a coronal flux rope can be obtained from eruption data (post-eruption arcade, LOS magnetogram, white-light CME) under the assumption of cylindrical force-free flux rope

Different Techniques for Measurement of Bz

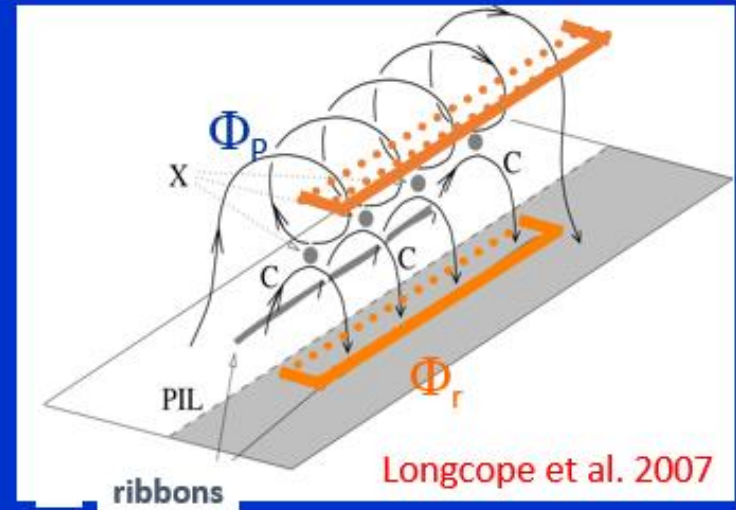
Fm N. Gopalswamy

CMEs

Background

- If CME flux ropes are formed during eruption, then the total reconnected (RC) flux (Φ_r) is same as the poloidal flux (Φ_p) of the resulting FR: $\Phi_r \approx \Phi_p$ (Longcope et al. 2007; Qiu et al. 2007; Hu et al. 2014; Gopalswamy et al. 2017)
- Φ_r can be computed using the photospheric B underlying cumulative ribbon area (Longcope et al. 2007; Qiu et al. 2007; Kazachenko et al. 2017)
- Φ_r can also be computed in a simpler way as half the flux underlying post eruption arcades (Gopalswamy et al. 2017)

- Coronal flux rope can be constructed using Φ_r and CME flux rope fit
- CME and flare properties closely related to Φ_r
- Coronal flux ropes can be tracked and compared with 1-au flux ropes



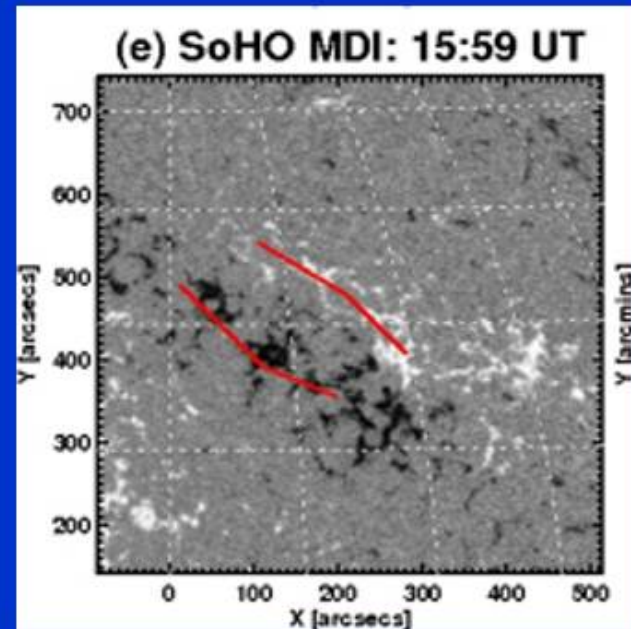
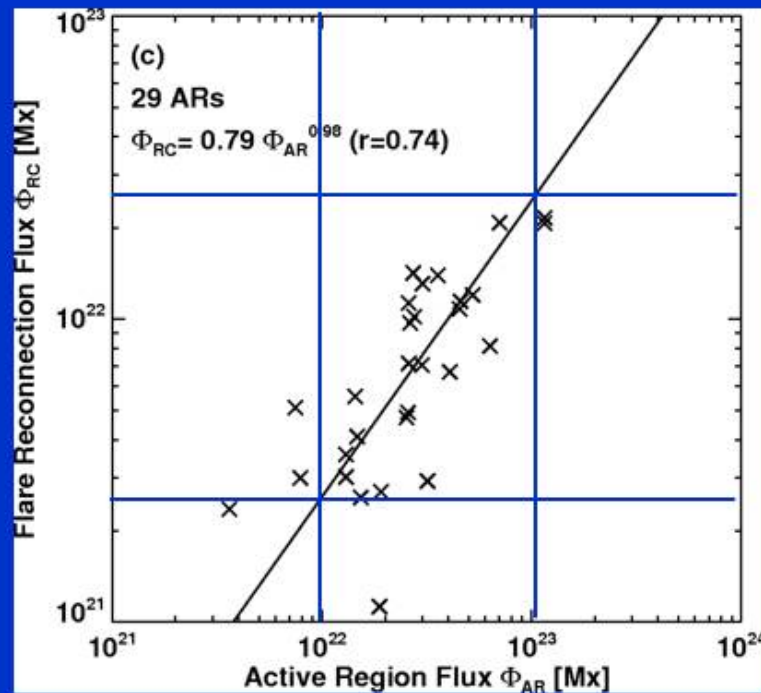
Different Techniques for Measurement of Bz

Fm N. Gopalswamy

CMEs

AR Flux vs. RC Flux

About 28% of AR flux is reconnected in an eruption

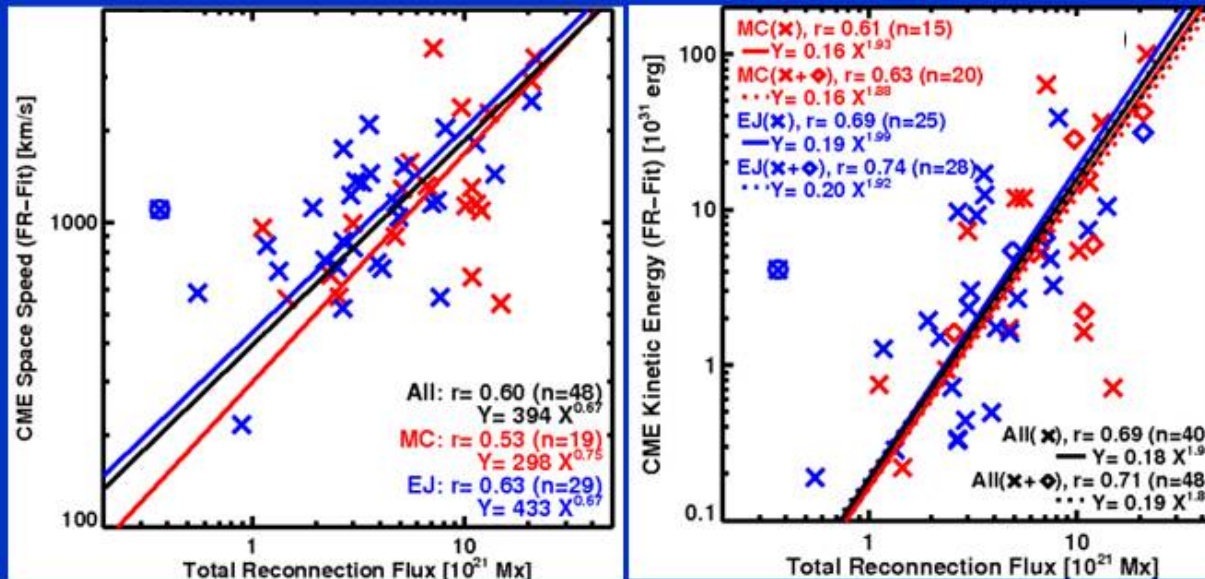


Different Techniques for Measurement of Bz

Fm N. Gopalswamy

CMEs

CME Speed and Kinetic Energy



- Both speed and kinetic energy of the CMEs are well correlated with the RC Flux ($r = 0.60, 0.69$)
- The higher the RC Flux, the faster are the CMEs
- KE has the second highest correlation with RC flux (the highest was with soft X-ray flare fluence)
- True when the CMEs ended up as MCs or ejecta

One event (2000 October 2) was excluded from the correlations because the arcade was ill-defined.

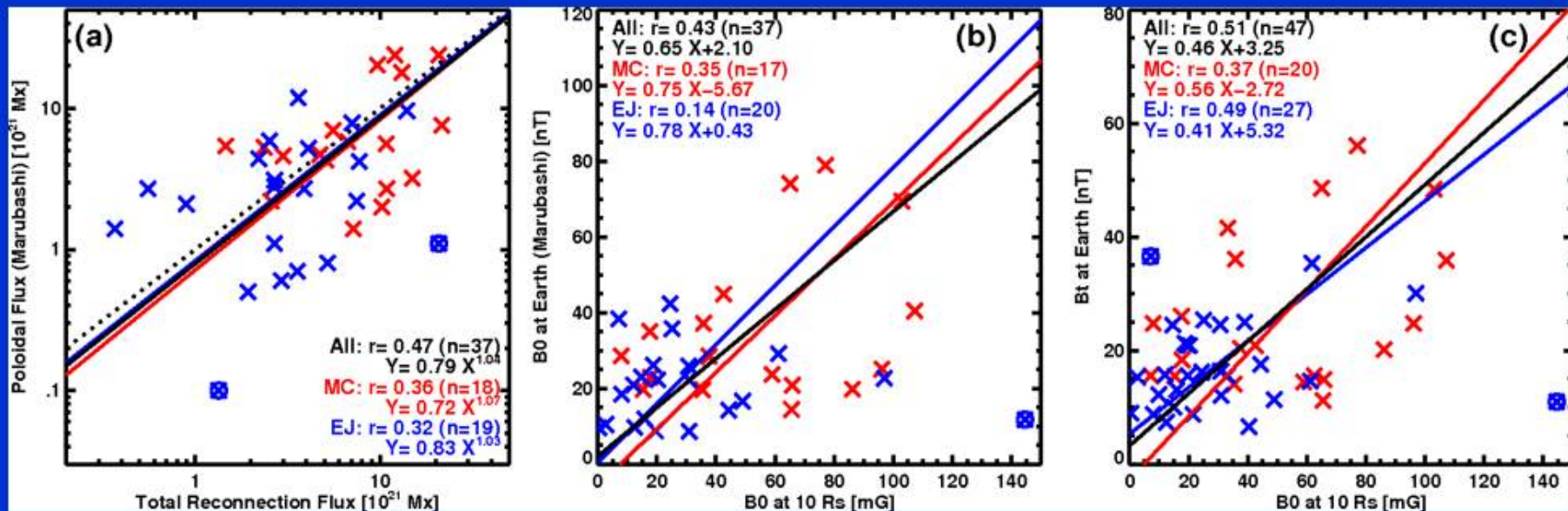
Diamonds – no mass data, so 10^{16} g assumed

Different Techniques for Measurement of Bz

Fm N. Gopalswamy

CMEs

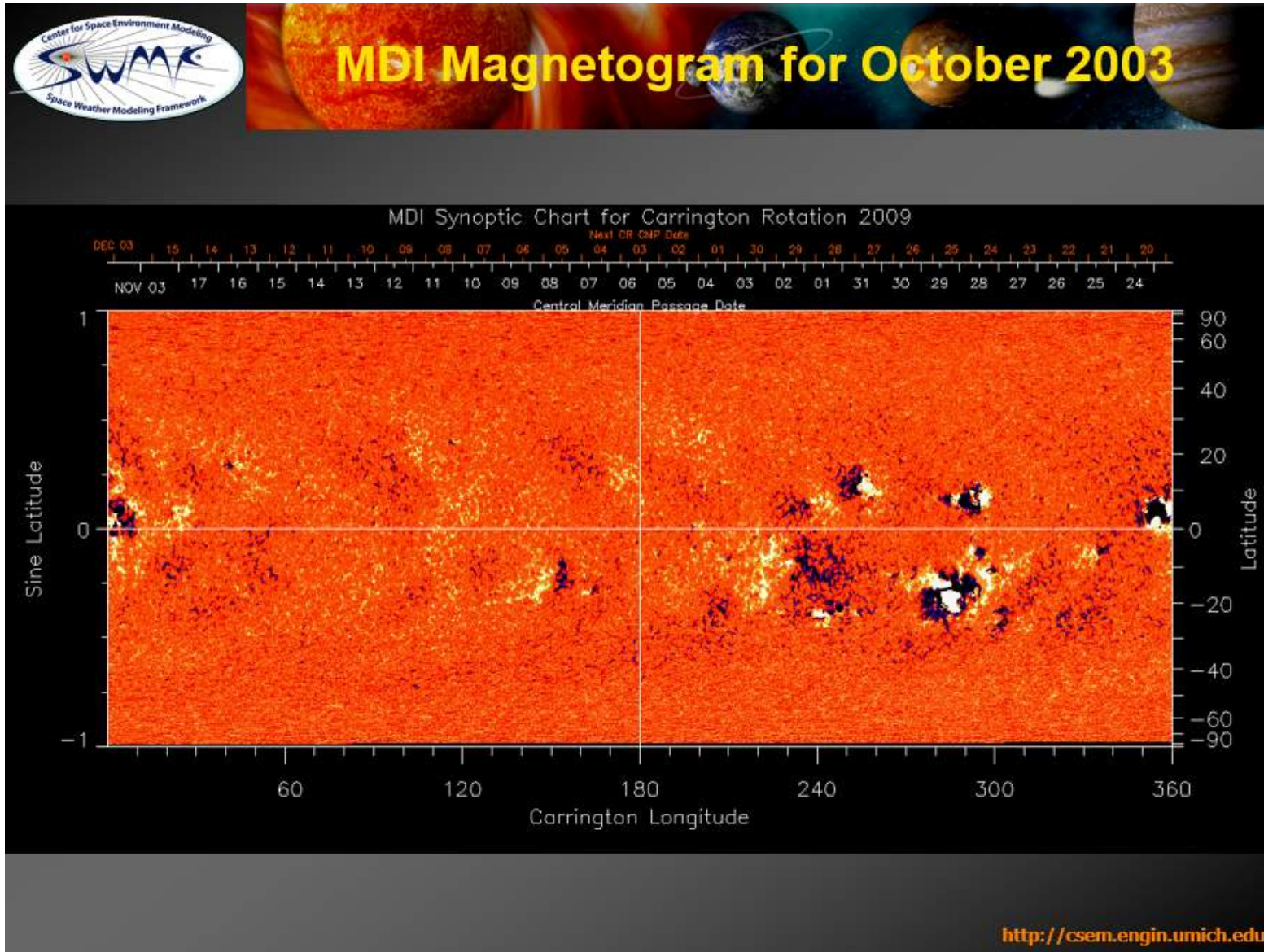
FR Properties at 1 au and 10 Rs are Correlated



The relation between RC flux and ICME poloidal flux confirms previous results obtained just for MCs
The relation between the axial field at the Sun obtained from eruption data and that from flux rope fit agree quite well; the correlation is better when actual peak ICME field is used.

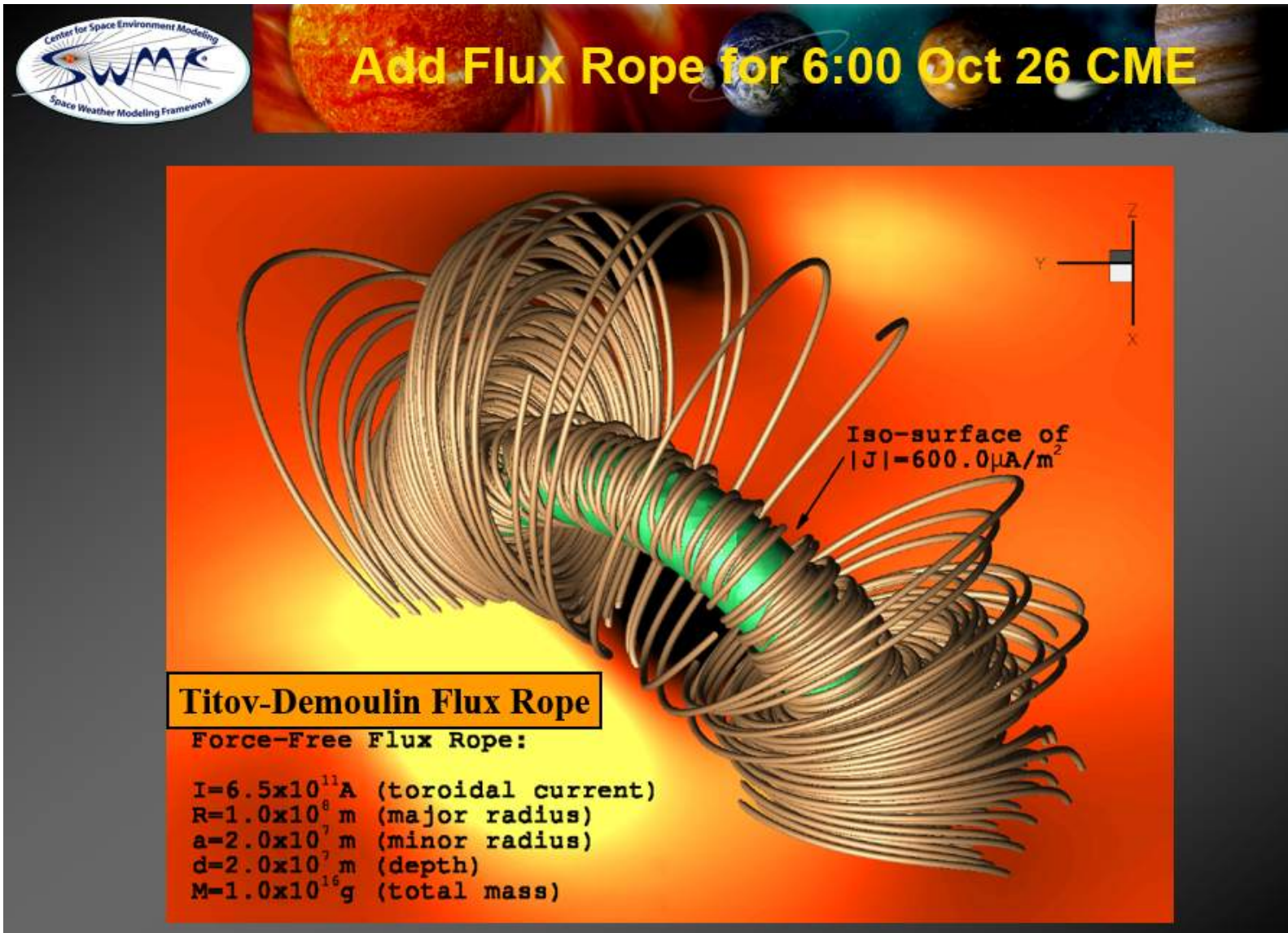
Different Techniques for Measurement of Bz

Fm Ward (Chip) Manchester **CMEs**



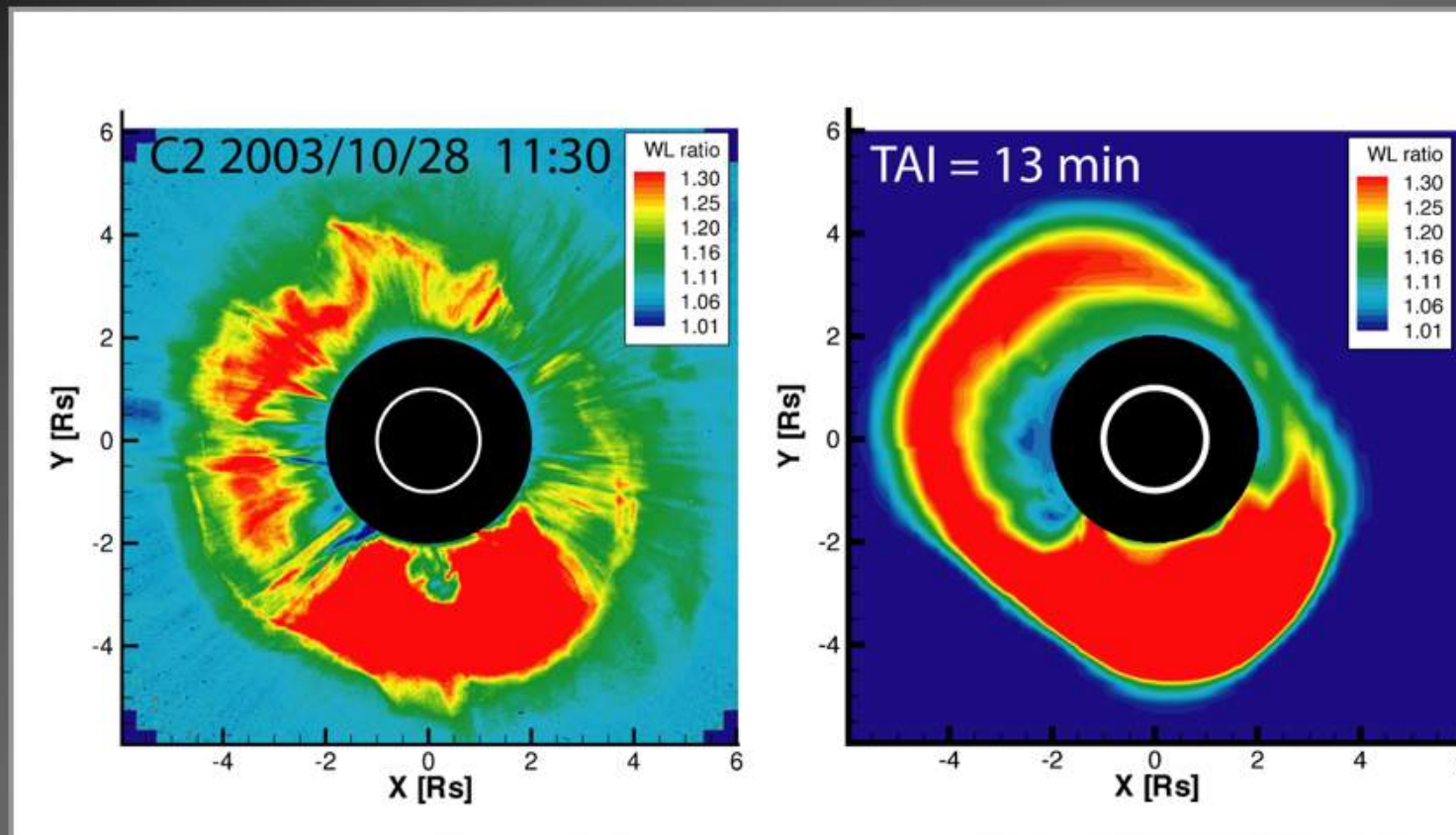
Different Techniques for Measurement of Bz

Fm Ward (Chip) Manchester **CMEs**



Different Techniques for Measurement of Bz

Fm Ward (Chip) Manchester **CMEs**



<http://csem.engin.umich.edu>

Different Techniques for Measurement of Bz

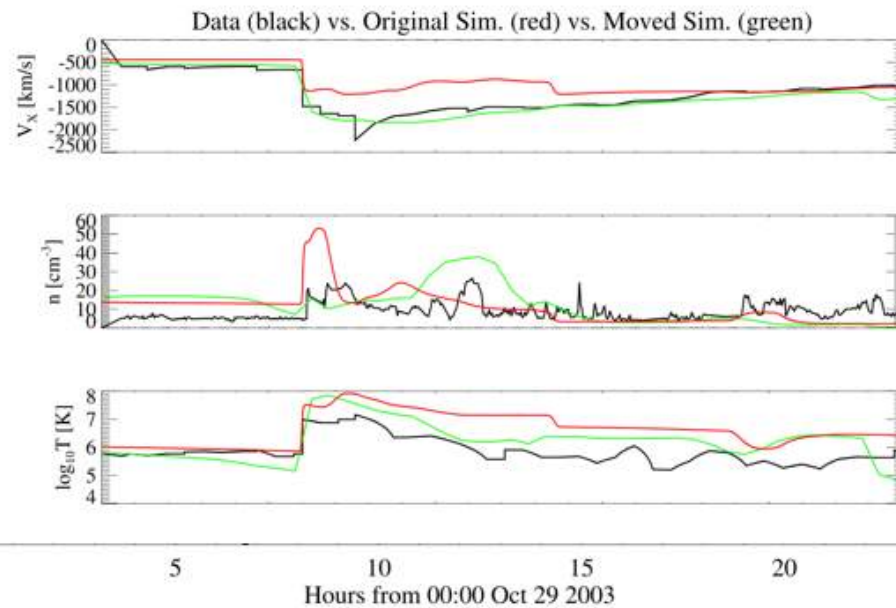
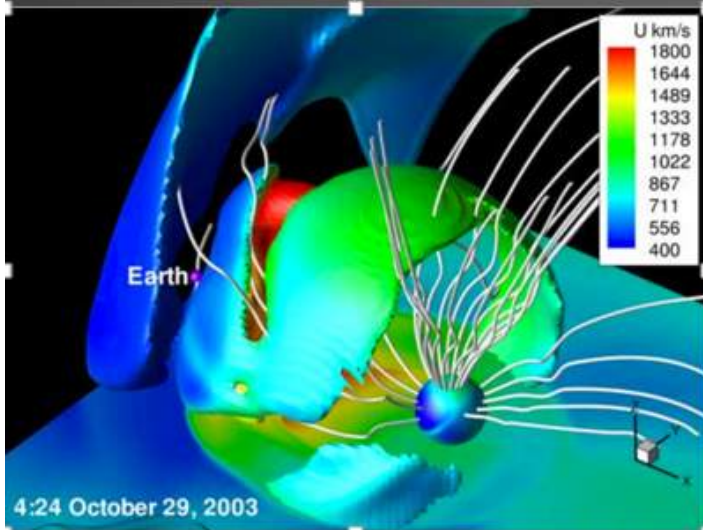
Fm Ward (Chip) Manchester **CMEs**



2003 Oct 28th CME Simulation

CME Simulation with the AWSoM Model:

- Titov-Demoulin flux rope erupts from active region 10486
- The simulation velocity is close but densities are too high.
- Arrival time shifted only 1.8 and 3.4 hours to match observations
- Green line shifted 9 degrees eastward



Toth et al. 2007
Manchester et al. 2008

<http://csem.engin.umich.edu>

Different Techniques for Measurement of Bz

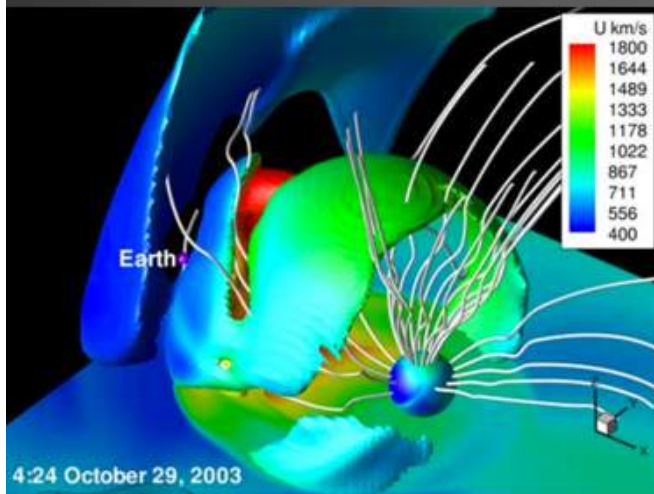
Fm Ward (Chip) Manchester **CMEs**



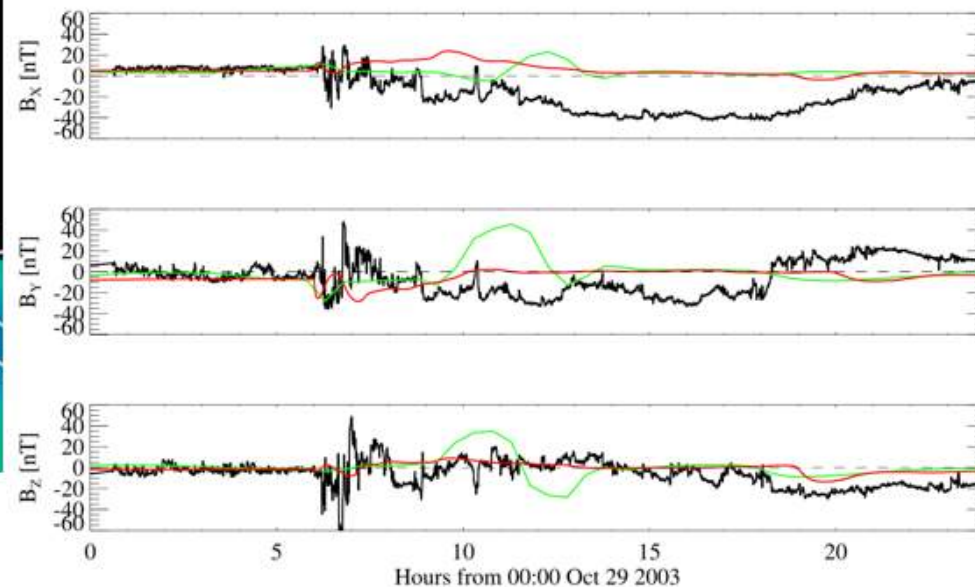
2003 Oct 28th CME Simulation

CME Simulation with the AWSOM Model:

- Titov-Demoulin flux rope erupts from active region 10486
- Magnetic cloud signatures at 1 AU including are not close to obs.



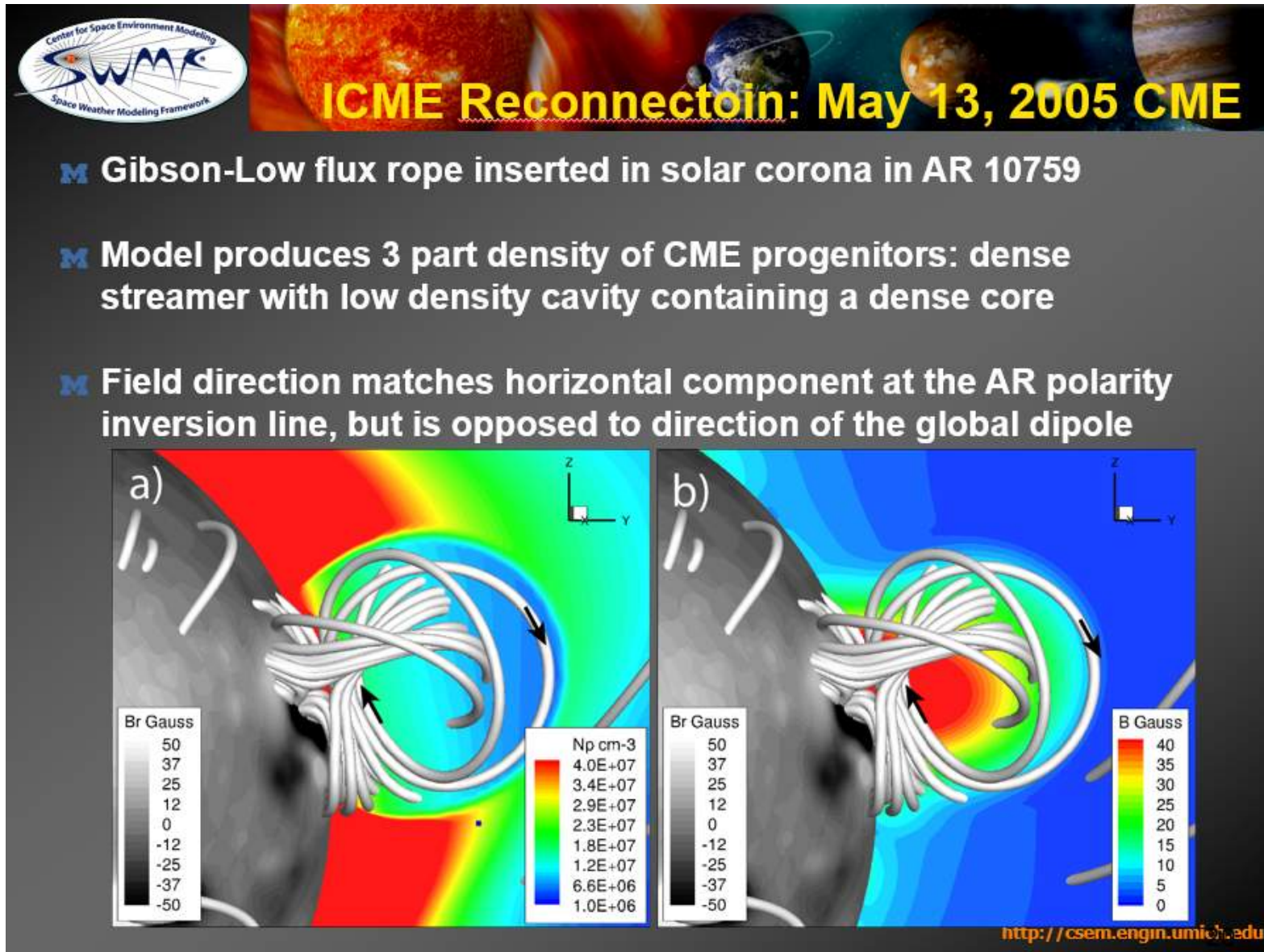
Toth et al. 2007
Manchester et al. 2008



<http://csem.engin.umich.edu>

Different Techniques for Measurement of Bz

Fm Ward (Chip) Manchester **CMEs**



Different Techniques for Measurement of Bz

Fm Ward (Chip) Manchester **CMEs**



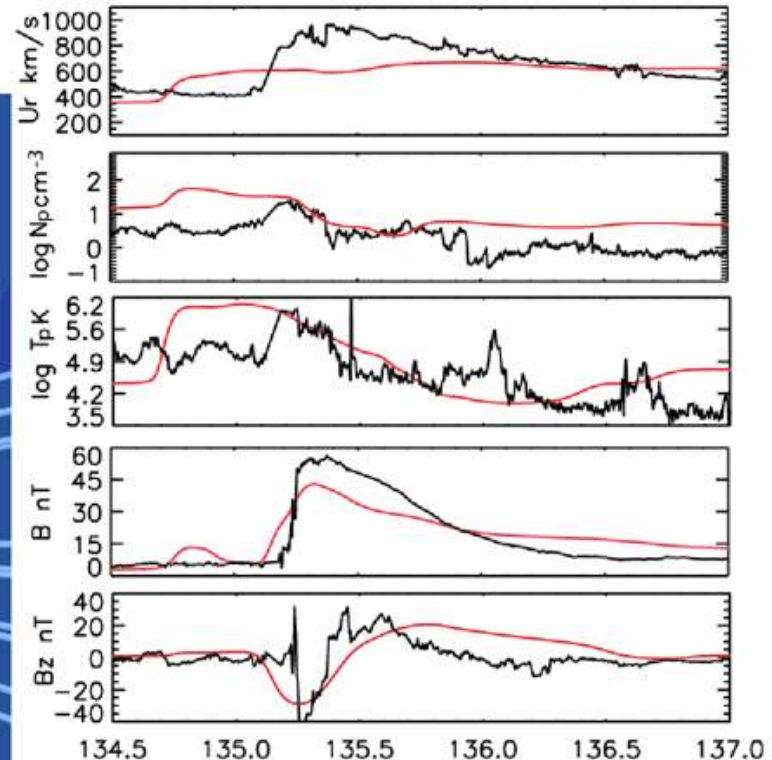
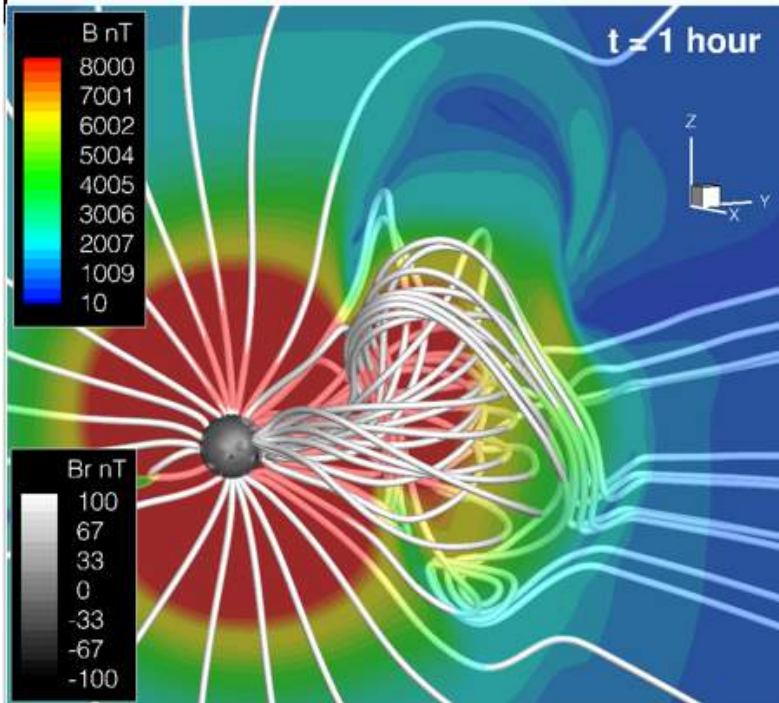
2005 May 13th CME Simulation

CME Simulation with the AWSoM Model:

- Gibson-Low flux rope erupts from active region 10759
- The simulation reproduces CME speed in corona
- The magnetic cloud signatures at 1 AU including the Bz rotation
- Shock Arrives 12 hours late
- Shift for comparison with B

Manchester, van der Holst & Lavraud, Plasma Phys. Control.

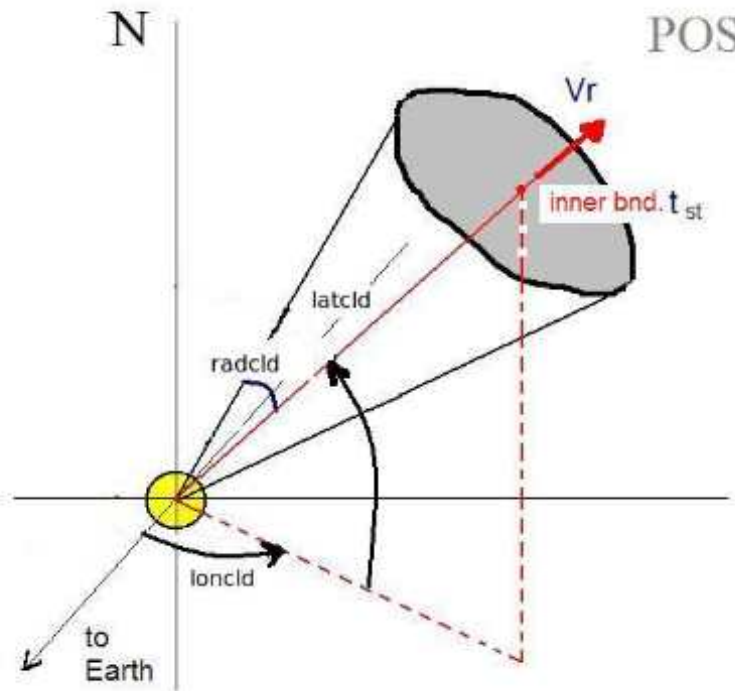
Fusion, 56, 2014



Different Techniques for Measurement of Bz

M. L. Mays & A. Taktakishvili **CMEs**

Cone model parameters



Input to ENLIL cone model run

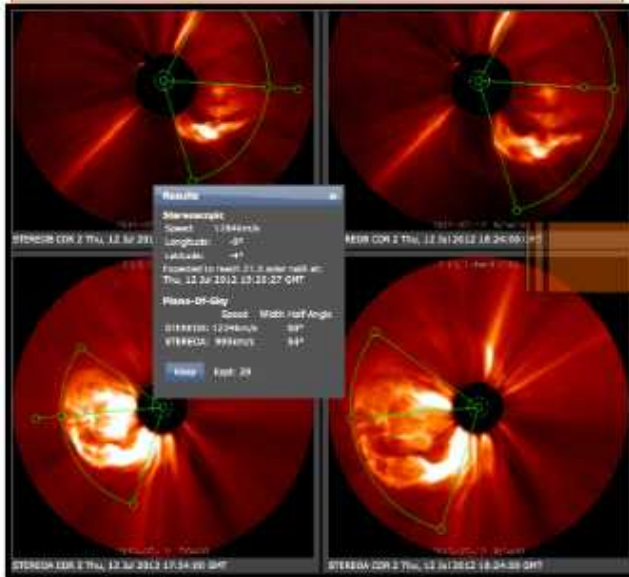
- time when cloud is at 21.5 Rs
- Latitude
- Longitude
- half-width
- Vr - radial velocity

Different Techniques for Measurement of Bz

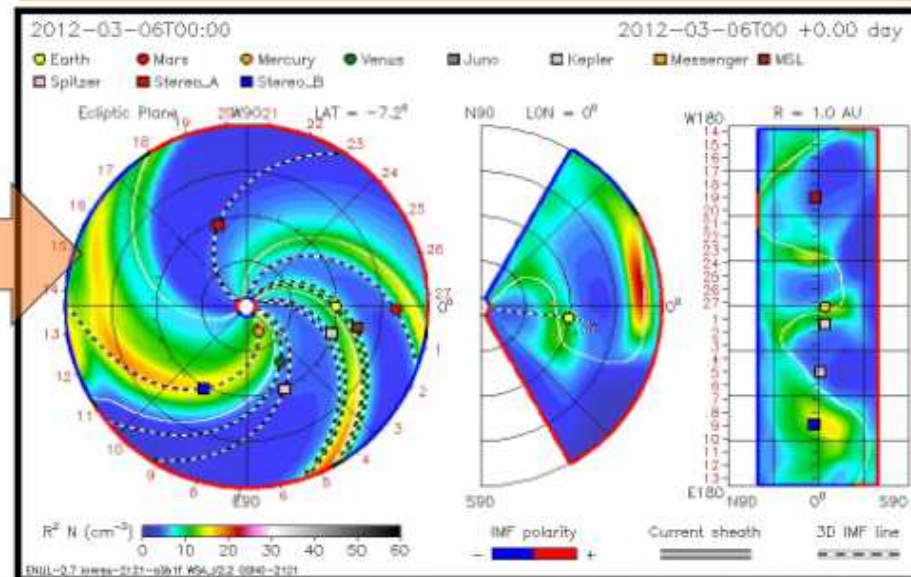
M. L. Mays & A. Taktakishvili **CMEs**

WSA-ENLIL Cone Model

Parameters Defined with
CCMC CME Triangulation
Tool



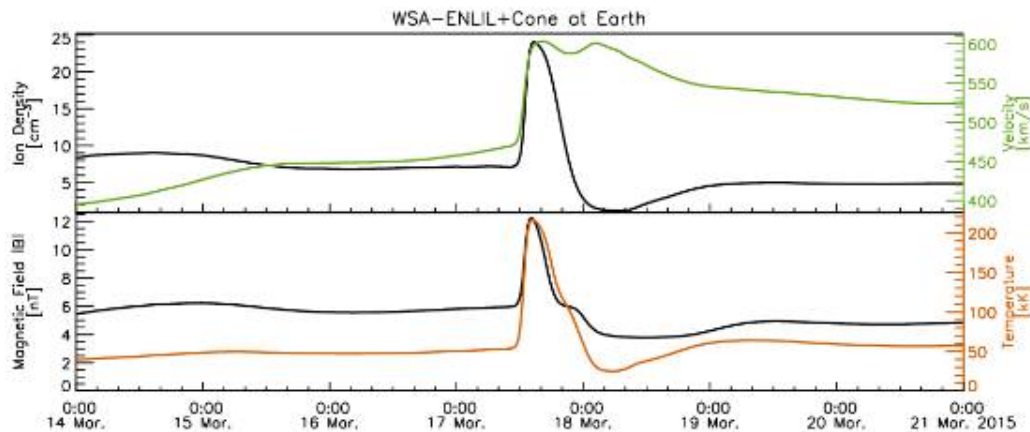
CME Parameters: Input To
WSA-ENLIL Cone Model



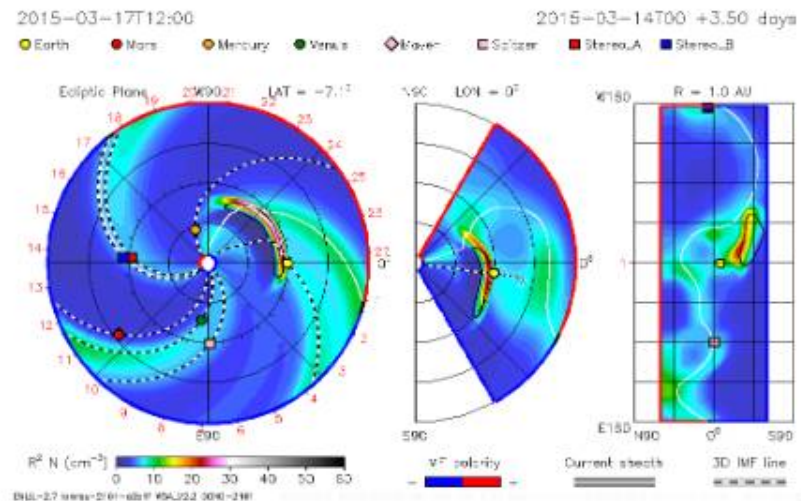
Different Techniques for Measurement of Bz

M. L. Mays & A. Taktakishvili **CMEs**

Determination of the CME Arrival Time – clear arrival



Timing and Field Amplitude sometimes good (state of the art)



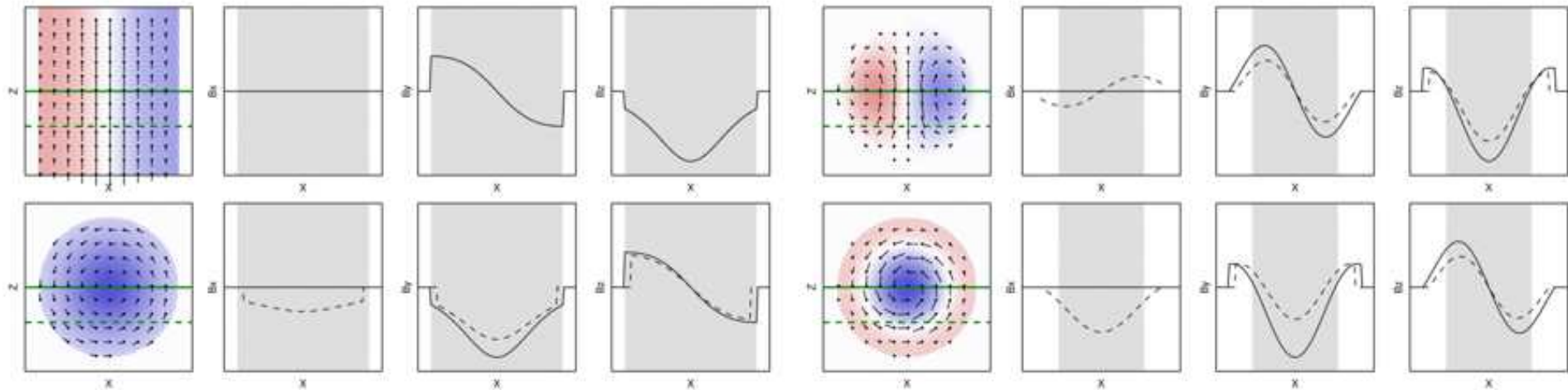
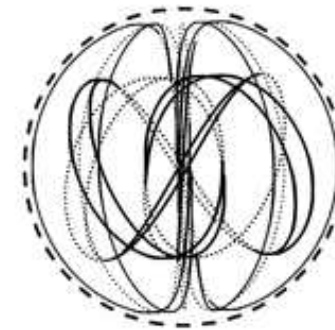
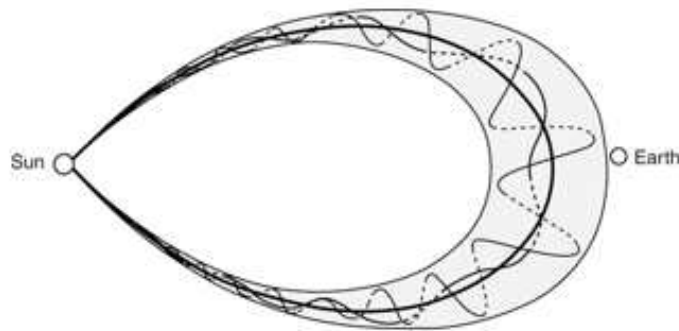
18

Different Techniques for Measurement of B_z

Fm Dusan Odstrcil

CMEs

Flux Rope vs Spheromak — Similar Magnetic Field Profiles



Numerical diffusion/erosion makes them even more similar (Savani)

Different Techniques for Measurement of Bz

Fm Dusan Odstrcil

CMEs

Simulated CME Events

date (yyyy-mm-dd)	2010-04-03	2012-07-12	2013-07-09
time (hh:mm)	15:00	16:54	15:09
lat (deg)	-25	-13	2
lon (deg)	0	6	-10
rmajor (deg)	40	55	40
vclد (km/s)	812	830	500
tilt (deg)	330	280	315
bcav (nT)	2500	3000	2500
hcav (-1 1)	1	1	-1
nclد (2 3)	2	2	2
dclد (x/dfast)	1	1	1
tclد (x/tfast)	1	1	1
radcav (x/rmajor)	0.8	0.8	0.8
dcav (x/dfast)	1	1	1
tcav (x/tfast)	1	1	1

Different Techniques for Measurement of Bz

Fm Dusan Odstrcil

CMEs

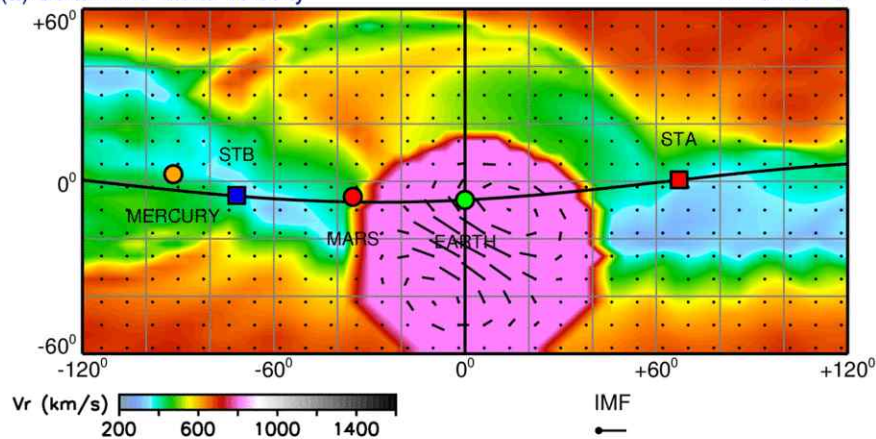
CME Event 2010-04-03 — Boundary Conditions

2010-04-03T18:39

2010-04-03T00 + 0.77 days

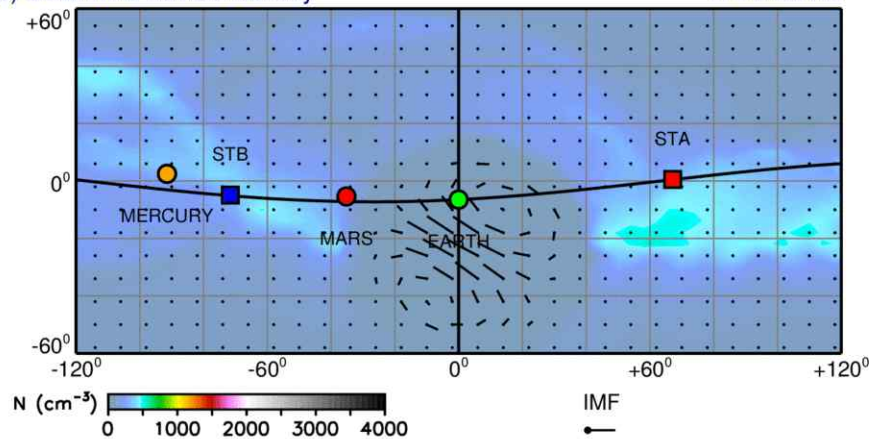
(a) Solar wind radial velocity

R = 0.100 AU



(b) Solar wind number density

R = 0.100 AU

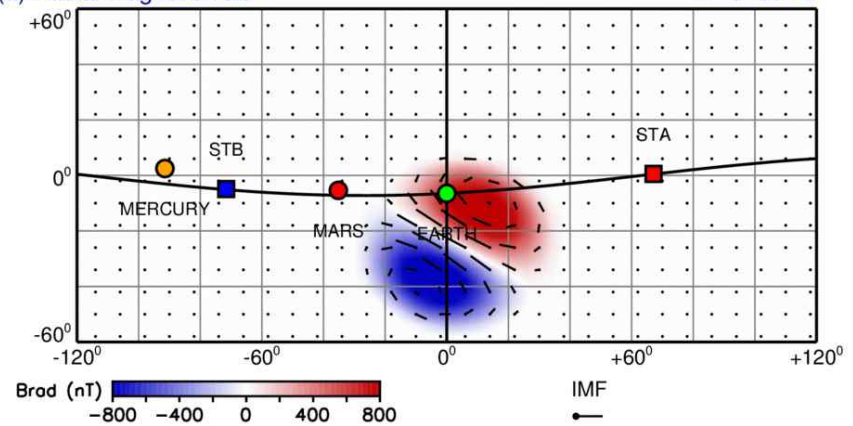


2010-04-03T18:39

2010-04-03T00 + 0.77 days

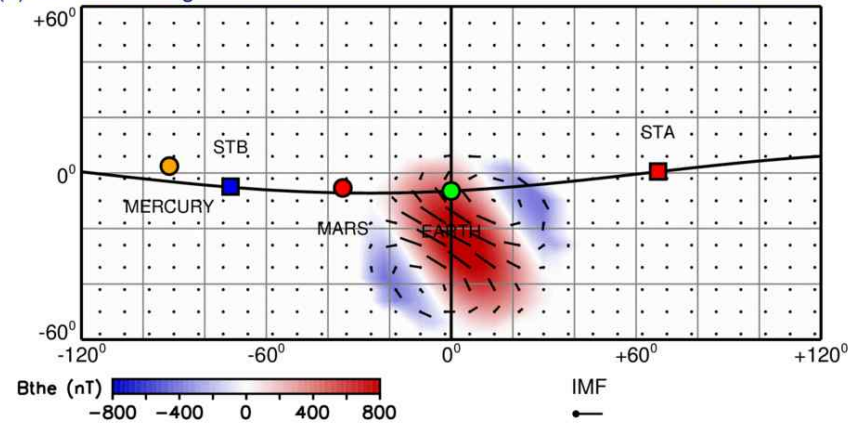
(a) Radial magnetic field

R = 0.100 AU



(b) Meridional magnetic field

R = 0.100 AU



ENLIL-lowres + GONGb-WSAdu + Spheromak / a9b0 / d1v812r40n2q-bp2500d1n330

HelioWeather

ENLIL-lowres + GONGb-WSAdu + Spheromak / a9b0 / d1v812r40n2q-bp2500d1n330

HelioWeather

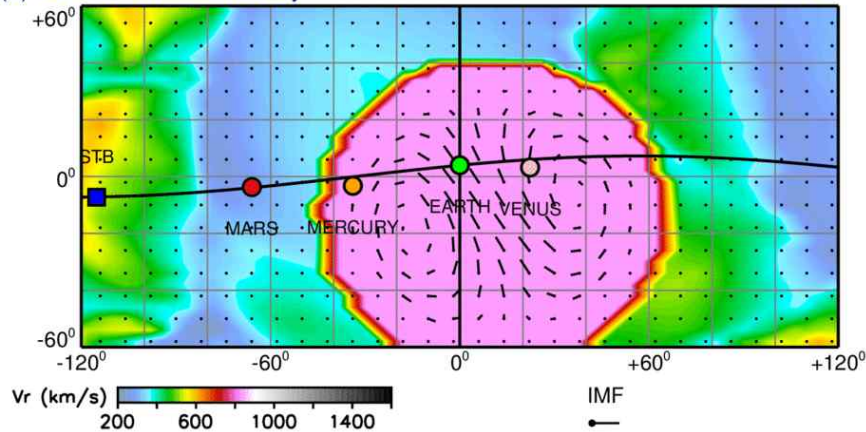
Different Techniques for Measurement of Bz

Fm Dusan Odstrcil

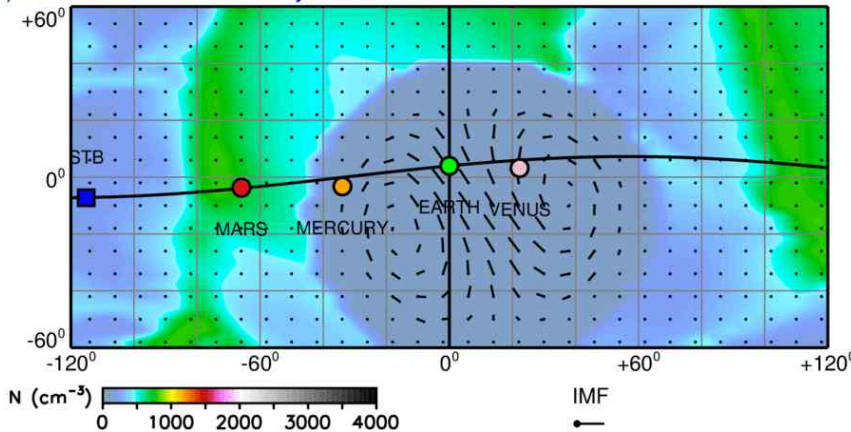
CMEs

CME Event 2012-07-12 — Boundary Conditions

2012-07-12T21:49 2012-07-12T00 + 0.90 days
 (a) Solar wind radial velocity R = 0.100 AU



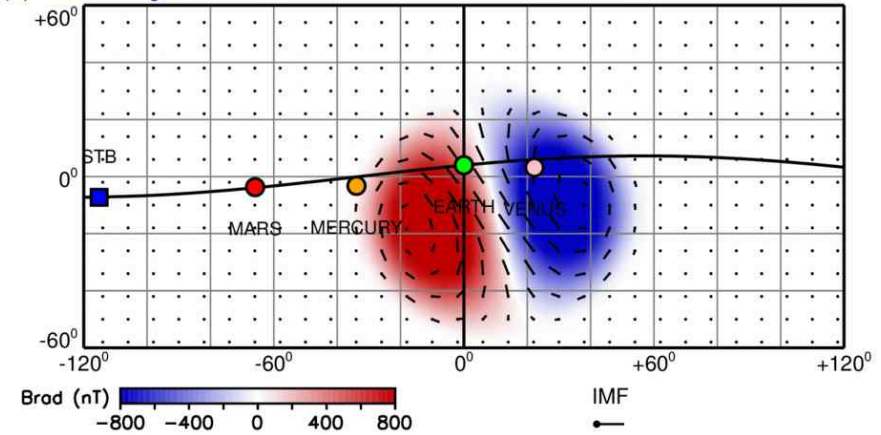
(b) Solar wind number density R = 0.100 AU



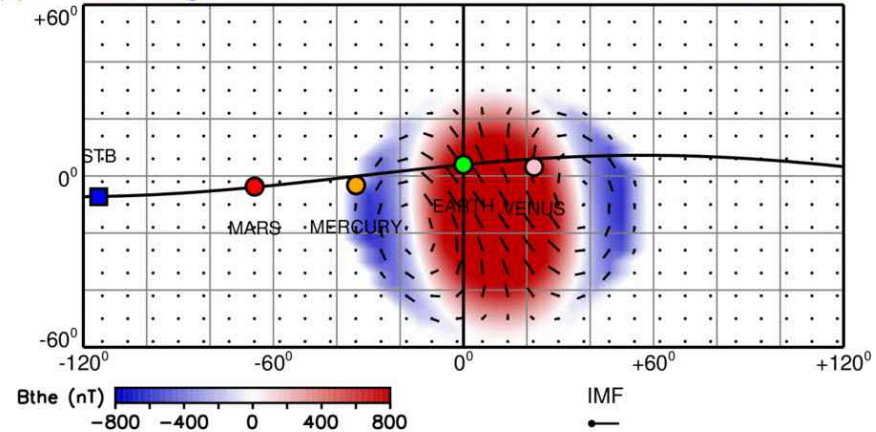
ENLIL-lowres + GONGb-WSAdu + Spheromak / a7b0 / d1v830r55n2q-bp3000d1p280

HelioWeather

2012-07-12T21:49 2012-07-12T00 + 0.90 days
 (a) Radial magnetic field R = 0.100 AU



(b) Meridional magnetic field R = 0.100 AU



ENLIL-lowres + GONGb-WSAdu + Spheromak / a7b0 / d1v830r55n2q-bp3000d1p280

HelioWeather

Different Techniques for Measurement of Bz

Fm Dusan Odstrcil

CMEs

CME Event 2013-07-09 — Boundary Changes

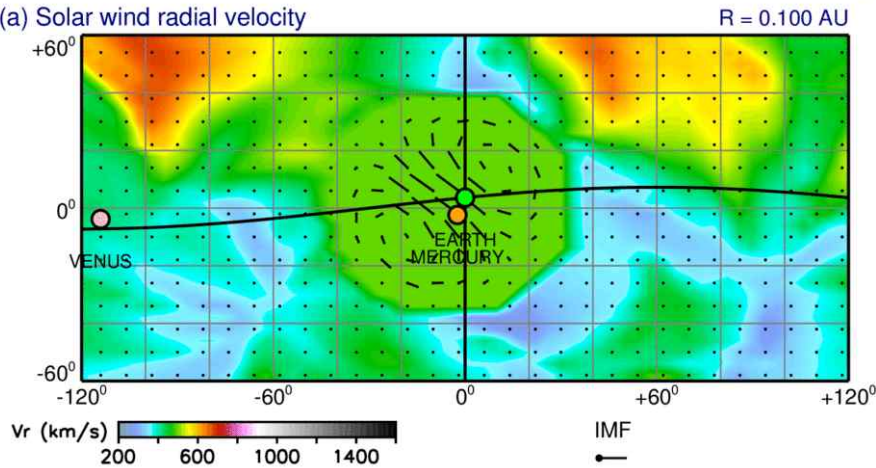
2013-07-09T21:06

2013-07-09T00 + 0.87 days

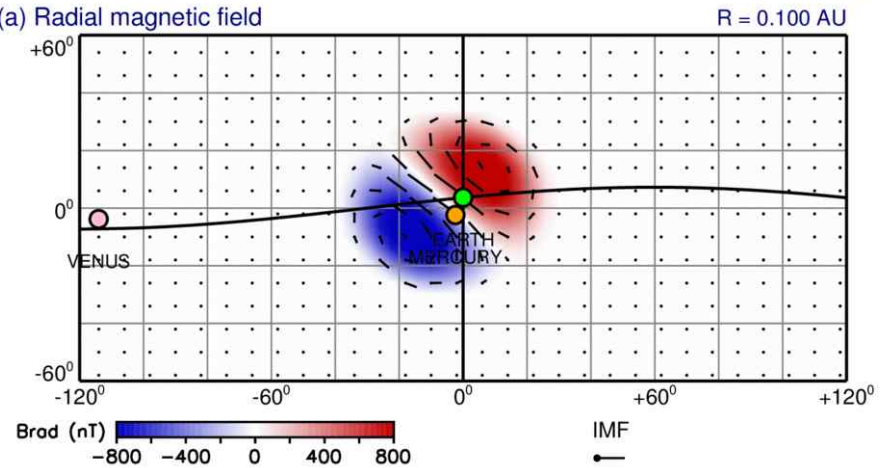
2013-07-09T21:06

2013-07-09T00 + 0.87 days

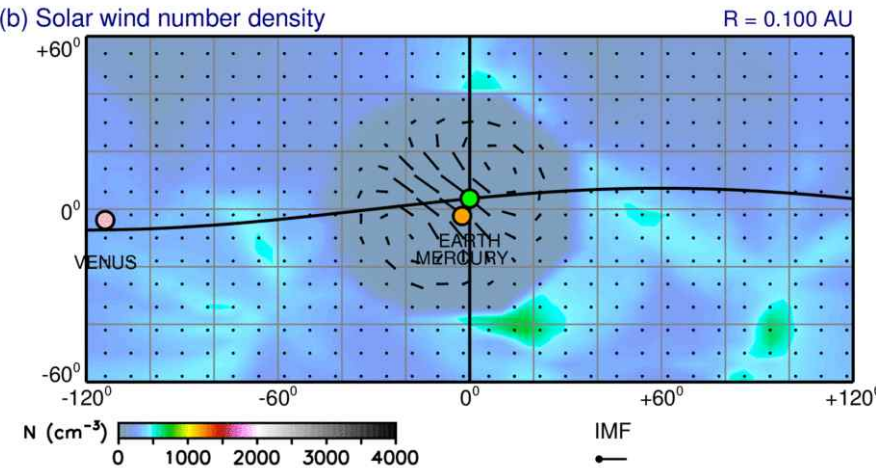
(a) Solar wind radial velocity



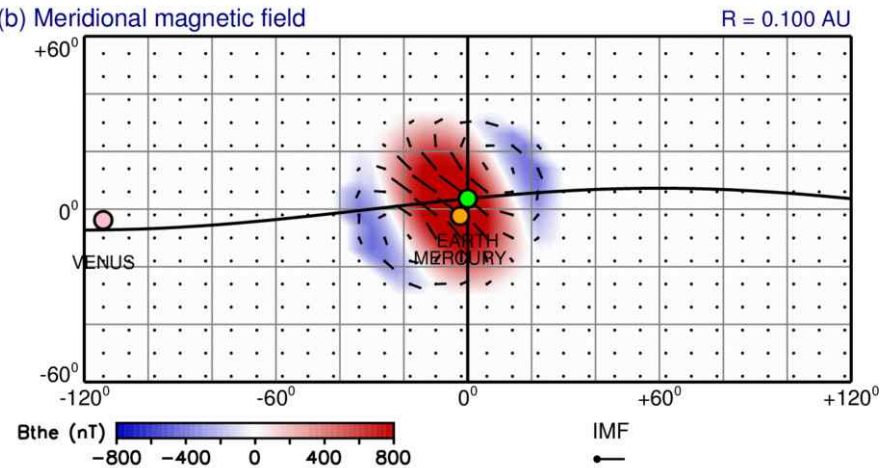
(a) Radial magnetic field



(b) Solar wind number density



(b) Meridional magnetic field

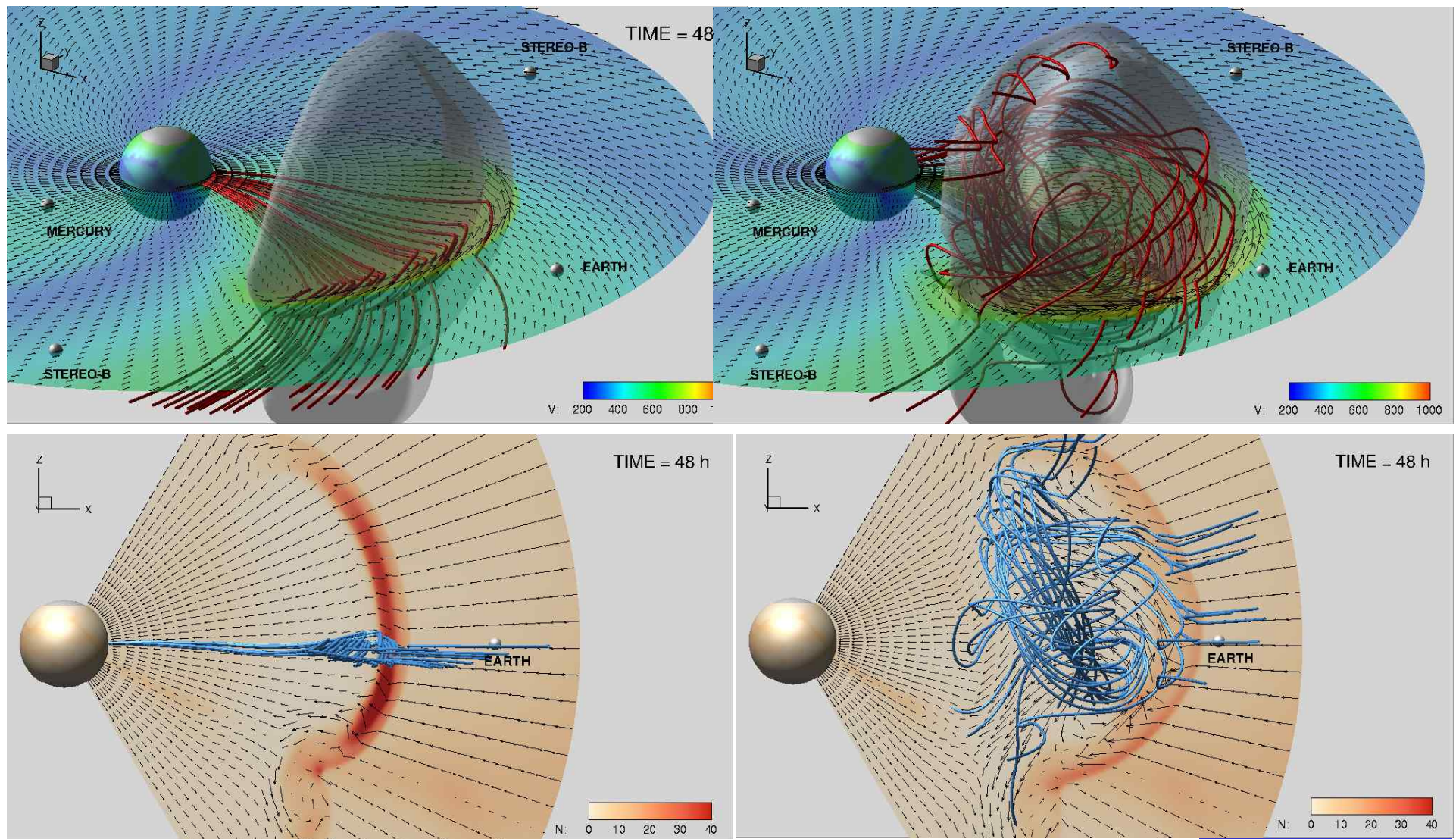


Different Techniques for Measurement of B_z

Fm Dusan Odstrcil

CMEs

2010-04-03 CME — “Cone” vs “Spheromak”

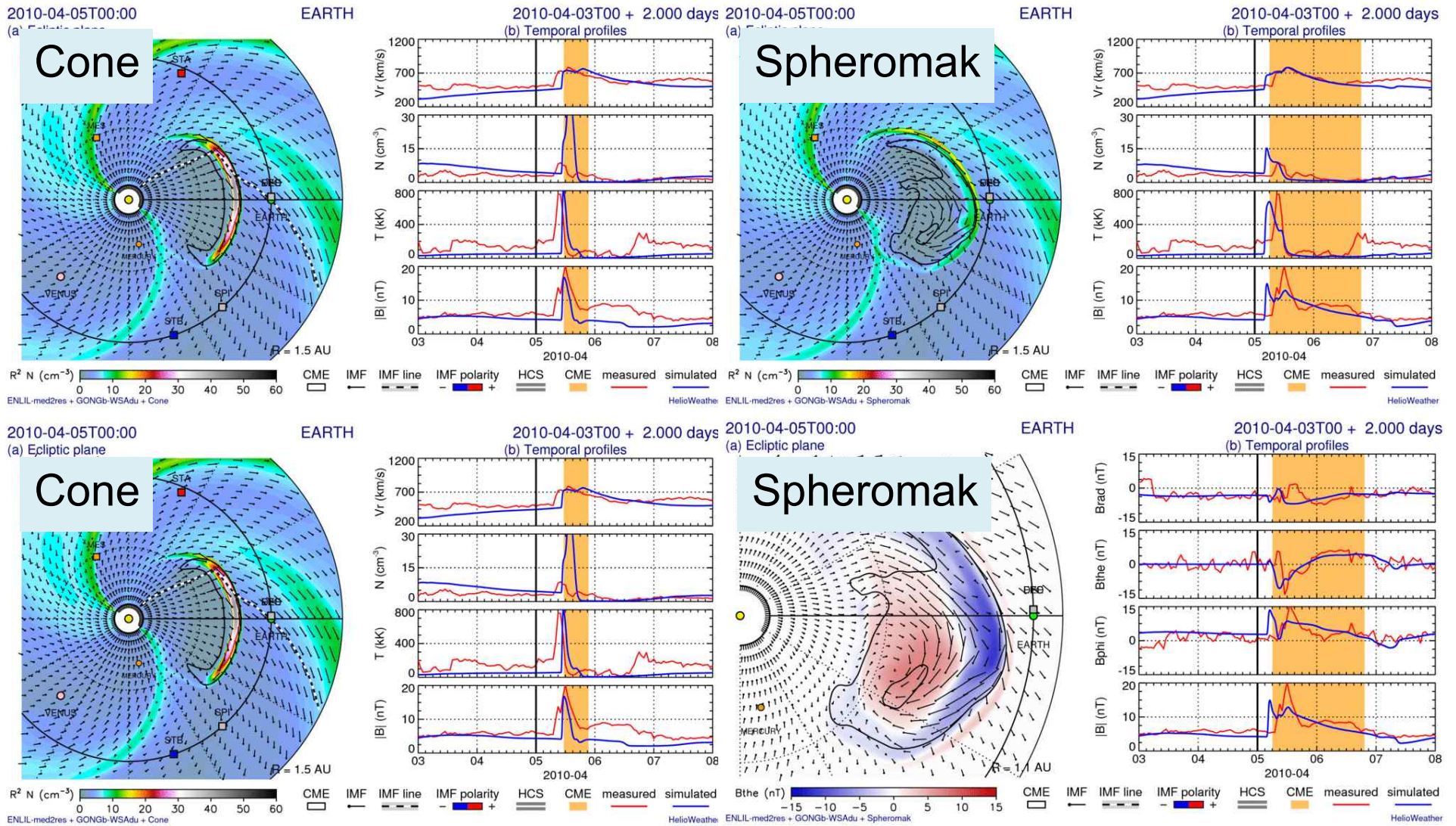


Different Techniques for Measurement of Bz

Fm Dusan Odstrcil

CMEs

2010-04-03 CME — “Cone” vs “Spheromak” density



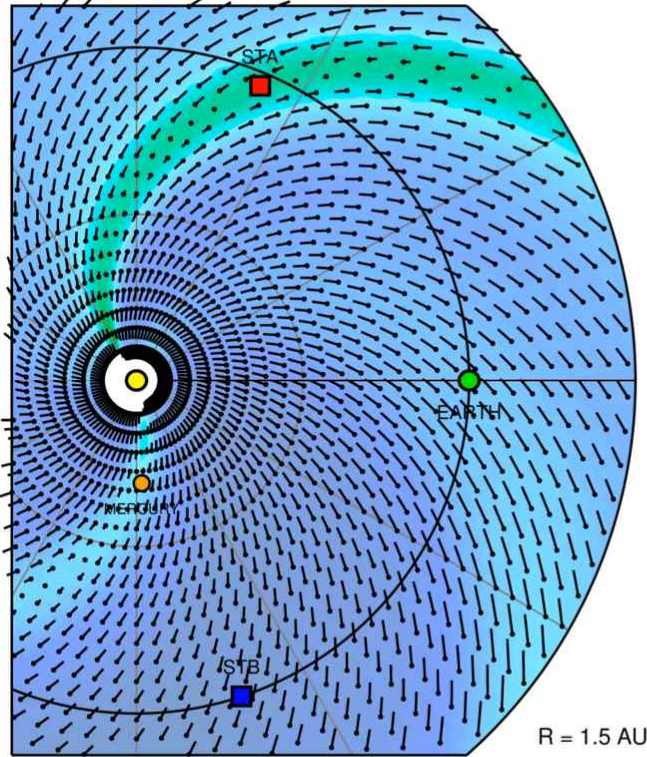
Different Techniques for Measurement of Bz

Fm Dusan Odstrcil

CMEs

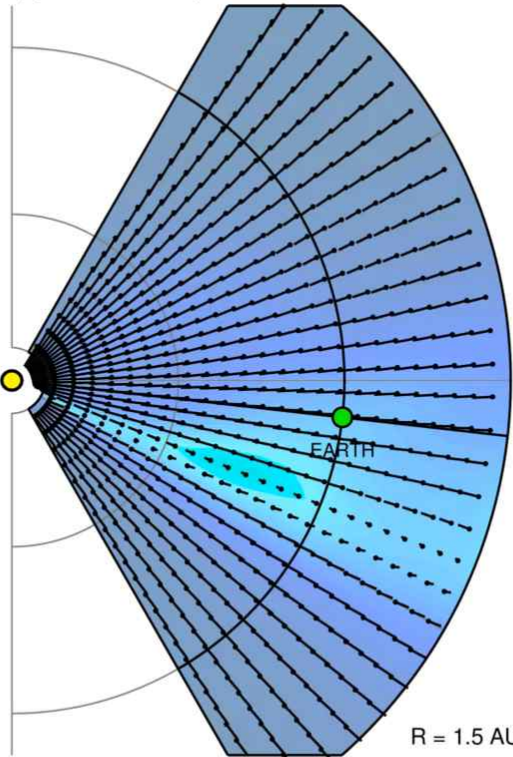
2010-04-03T00:00

(a) Ecliptic plane



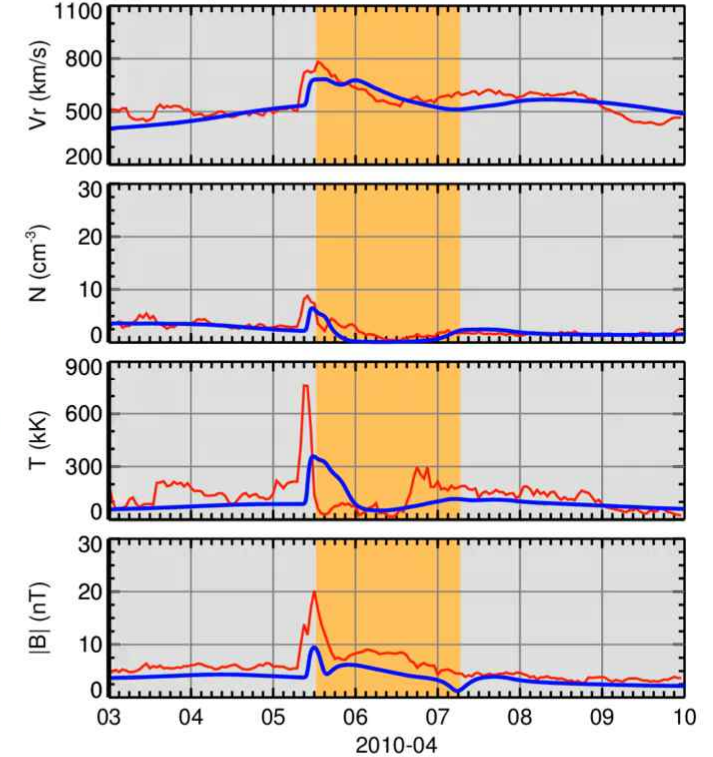
EARTH

(b) Meridional plane



2010-04-03T00 + 0.000 days

(c) Temporal profiles



ENLIL-lowres + GONGb-WSAdU + Spheromak / b9b1 / d1v850r40n2q-bp3000d1n330 / g53h10b04 / mc1um1d

CME sim obs
HeliWeather

Density

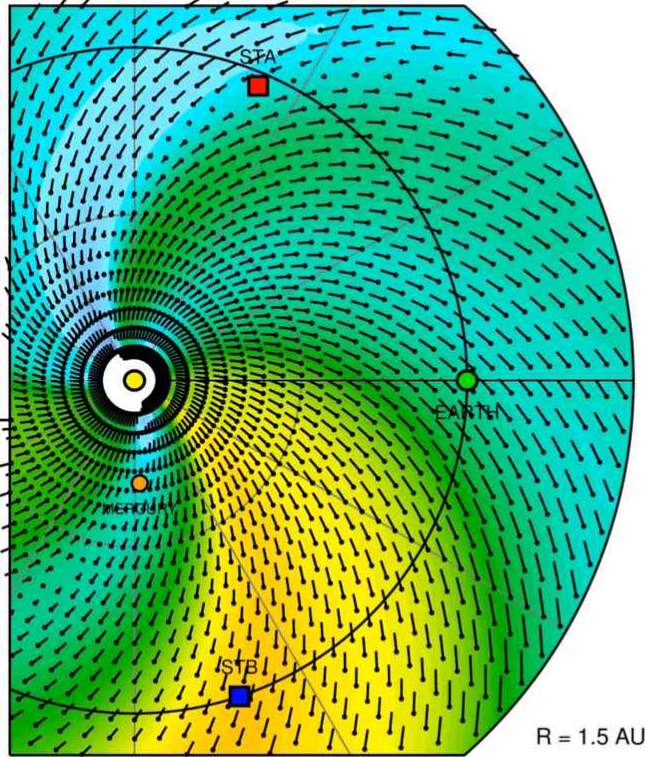
Different Techniques for Measurement of Bz

Fm Dusan Odstrcil

CMEs

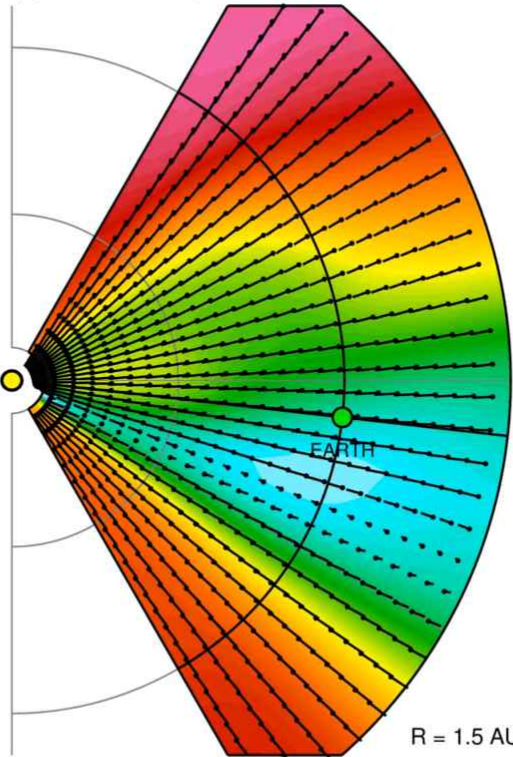
2010-04-03T00:00

(a) Ecliptic plane



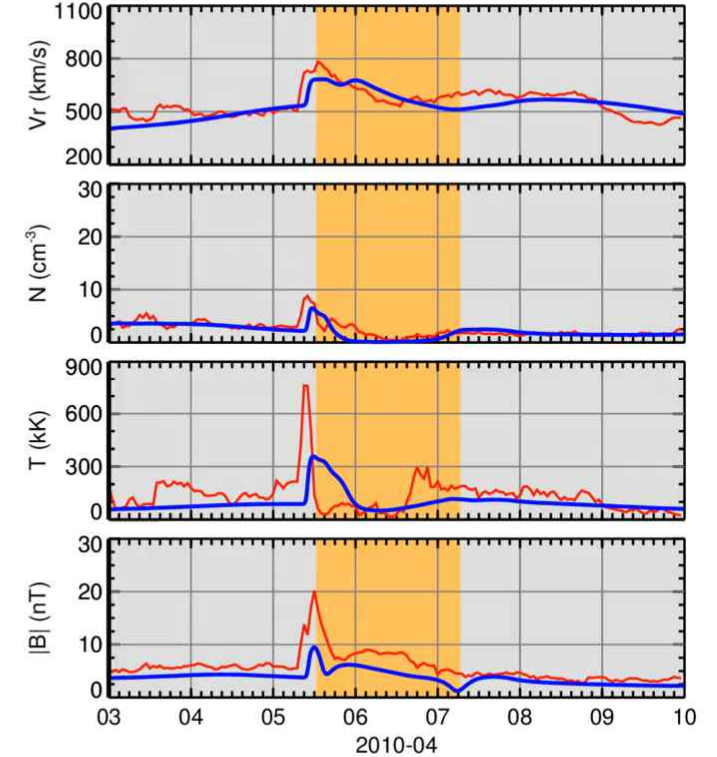
EARTH

(b) Meridional plane



2010-04-03T00 + 0.000 days

(c) Temporal profiles



ENLIL-lowres + GONGb-WSAdu + Spheromak / b9b1 / d1v850r40n2q-bp3000d1n330 / g53h10b04 / mc1um1d

CME sim obs
HeliWeather

Velocity

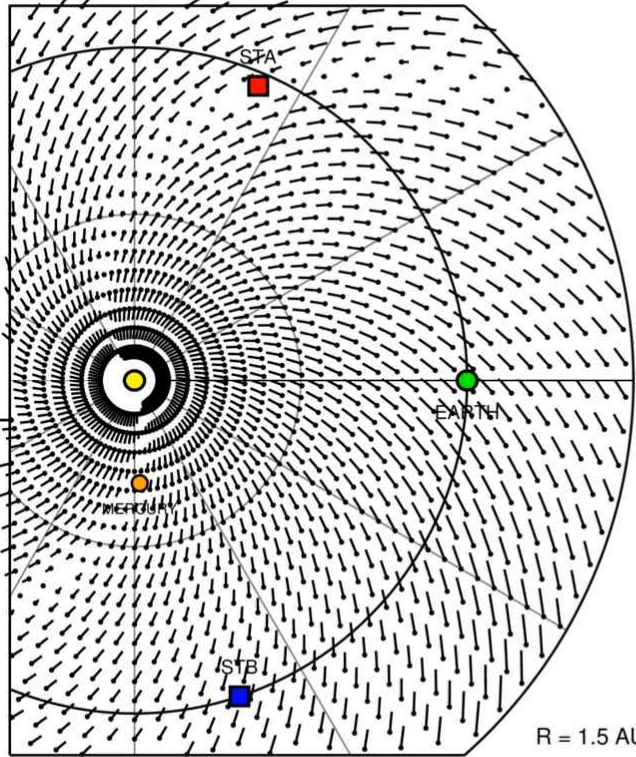
Different Techniques for Measurement of Bz

CMEs

Fm Dusan Odstrcil

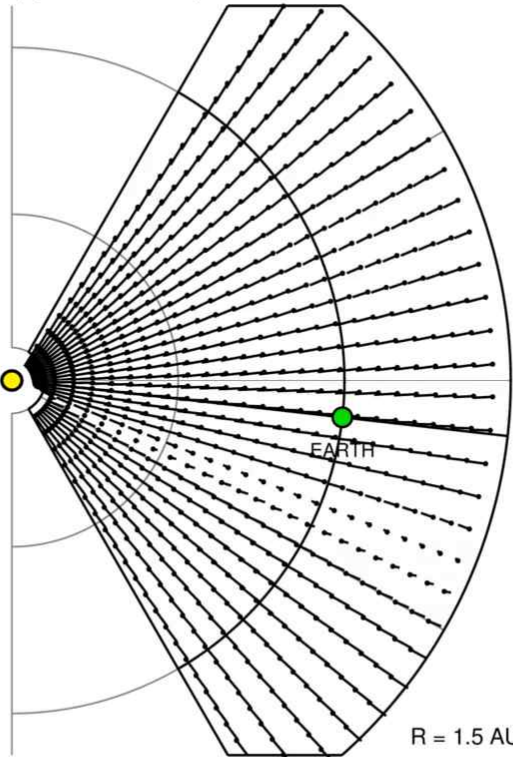
2010-04-03T00:00

(a) Ecliptic plane



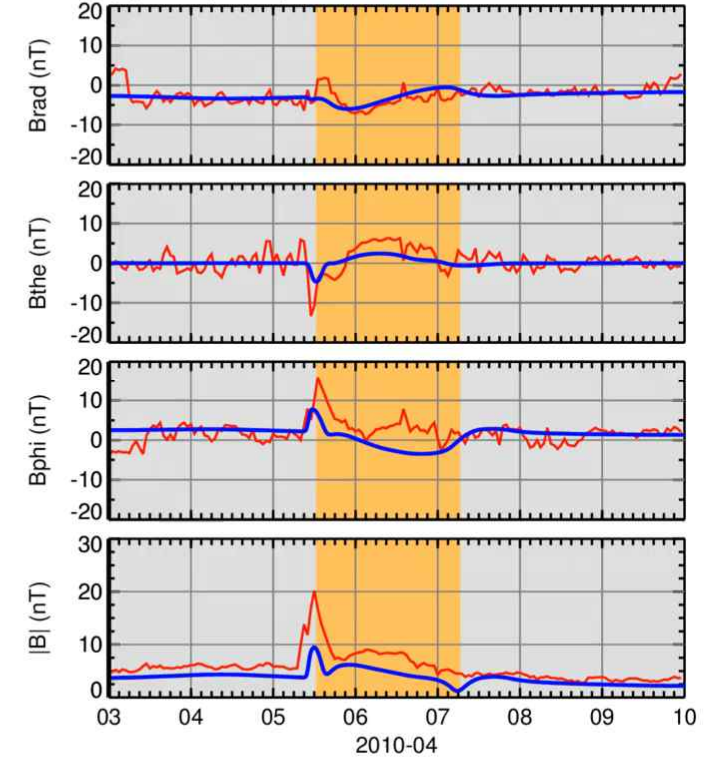
EARTH

(b) Meridional plane



2010-04-03T00 + 0.000 days

(c) Temporal profiles



ENLIL-lowres + GONGb-WSAdU + Spheromak / b9b1 / d1v850r40n2q-bp3000d1n330 / g53h10b04 / mc1um1d

HelioWeather

Magnetic Field B_{θ}

Different Techniques for Measurement of Bz

Heliospheric Remote Sensing

IPS Heliospheric Analyses ISEE (STELab)



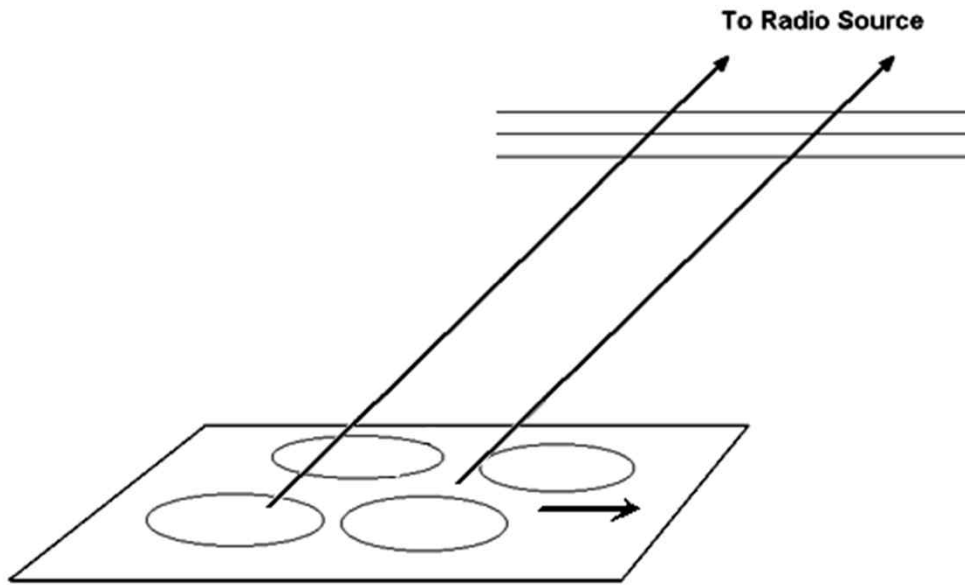
ISEE IPS array near Mt. Fuji



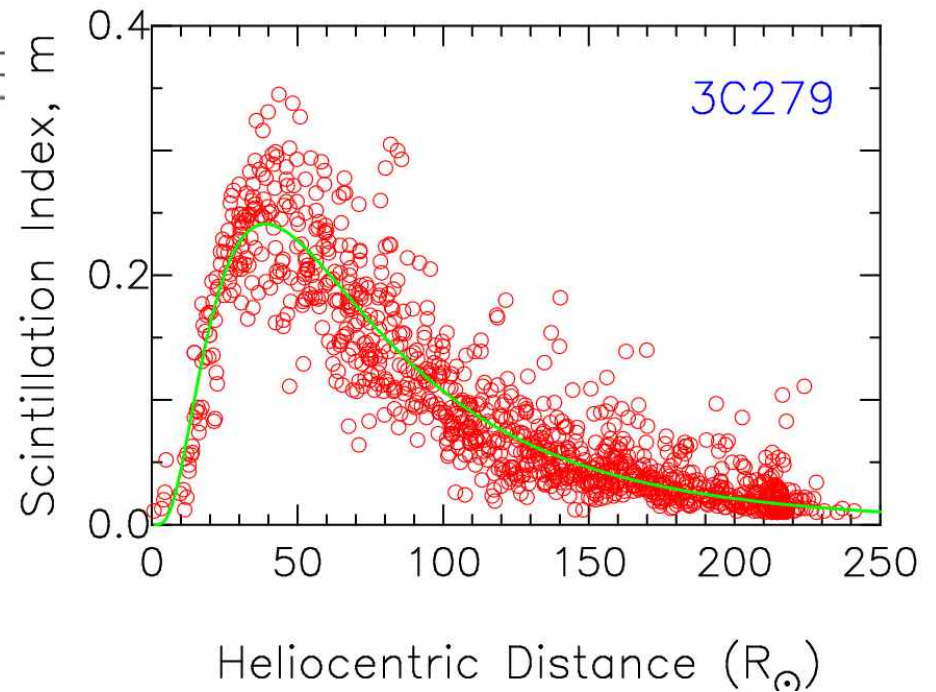
ISEE IPS array systems

Different Techniques for Measurement of Bz Heliospheric Remote Sensing

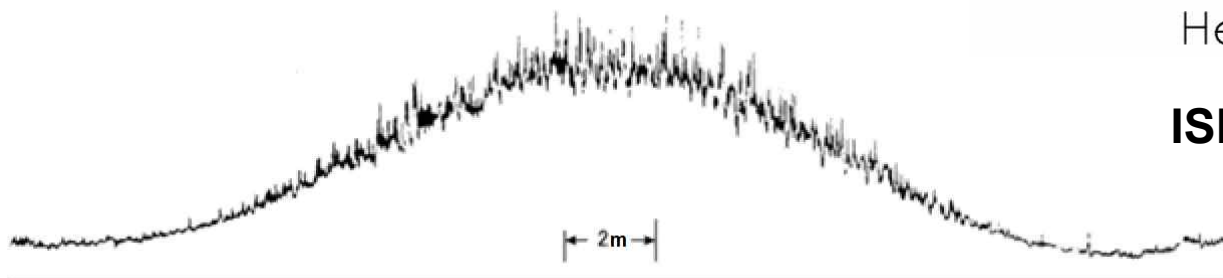
IPS Heliospheric Analyses ISEE (STELab)



IPS line-of-sight response



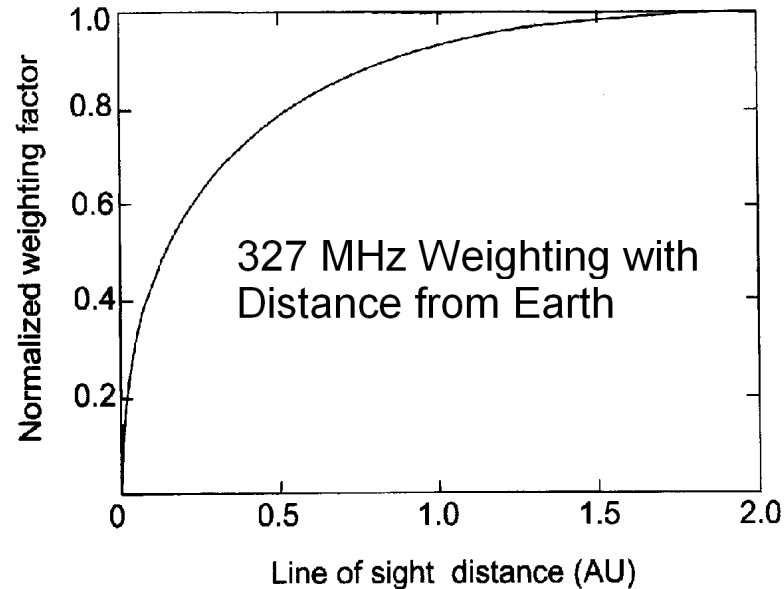
ISEE IPS array systems



Different Techniques for Measurement of Bz Heliospheric Remote Sensing

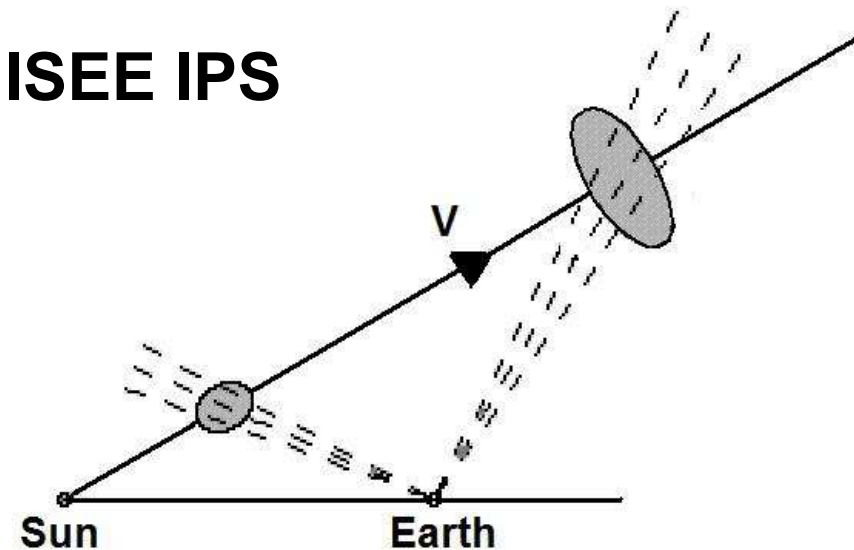
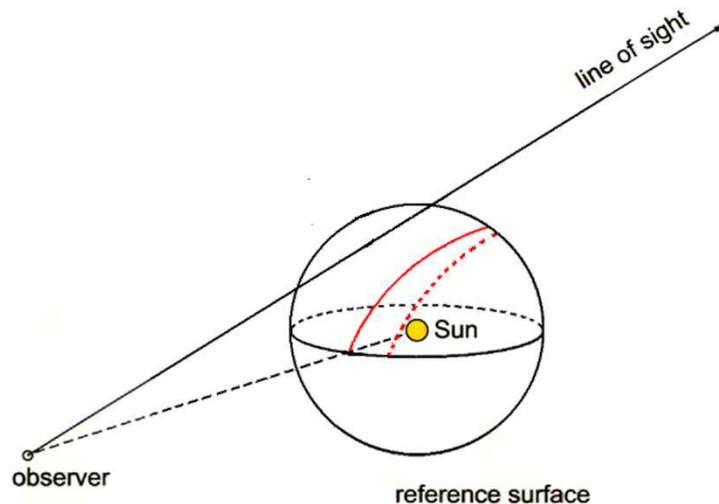
IPS line-of-sight response

Jackson, B.V., et al., 2008, *Adv. in Geosciences*, 21, 339-360.



Heliospheric C.A.T. analyses:
example line-of-sight distribution
for each sky location to form the
source surface of the 3D
reconstruction.

ISEE IPS



**Sample outward motion
over time**

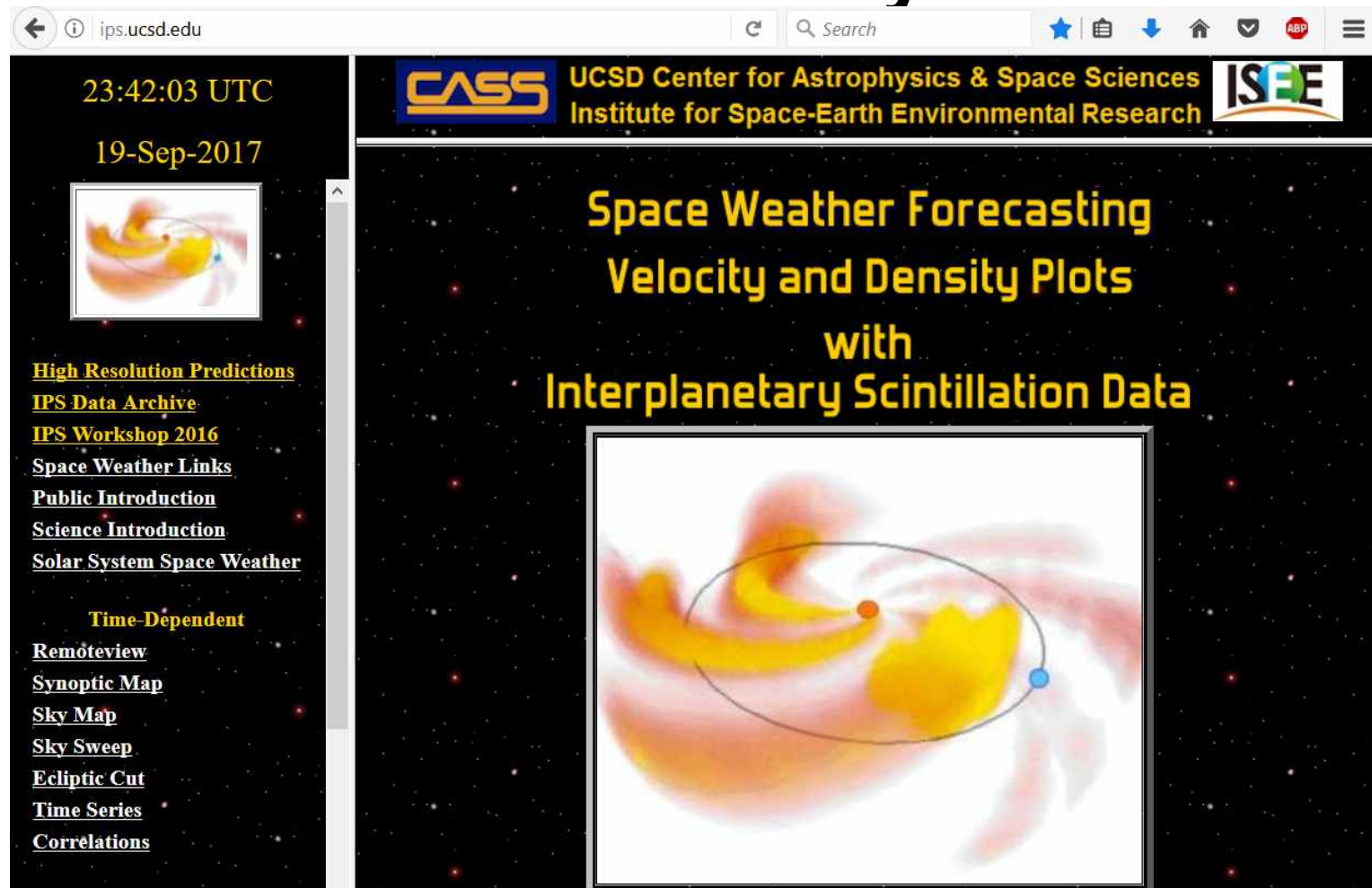
Different Techniques for Measurement of Bz Heliospheric Remote Sensing

Jackson, B.V., et al., 2011, *Adv. in Geosciences*, 30, 93-115.

<http://ips.ucsd.edu/> or http://ips.ucsd.edu/ips_workshop_2016/

UCSD Prediction Analyses

UCSD
Web
pages



The screenshot shows a web browser window with the URL ips.ucsd.edu. The page header includes the CASS logo (UCSD Center for Astrophysics & Space Sciences) and the ISEE logo (Institute for Space-Earth Environmental Research). The main content area features a large plot titled "Space Weather Forecasting Velocity and Density Plots with Interplanetary Scintillation Data". The plot shows a 3D visualization of the solar wind structure, with a central yellow region and surrounding pink and white structures. A blue dot and a red dot are visible on the plot. The left sidebar contains a navigation menu with the following items: "23:42:03 UTC", "19-Sep-2017", "High Resolution Predictions", "IPS Data Archive", "IPS Workshop 2016", "Space Weather Links", "Public Introduction", "Science Introduction", "Solar System Space Weather", "Time-Dependent", "Remoteview", "Synoptic Map", "Sky Map", "Sky Sweep", "Ecliptic Cut", "Time Series", and "Correlations".

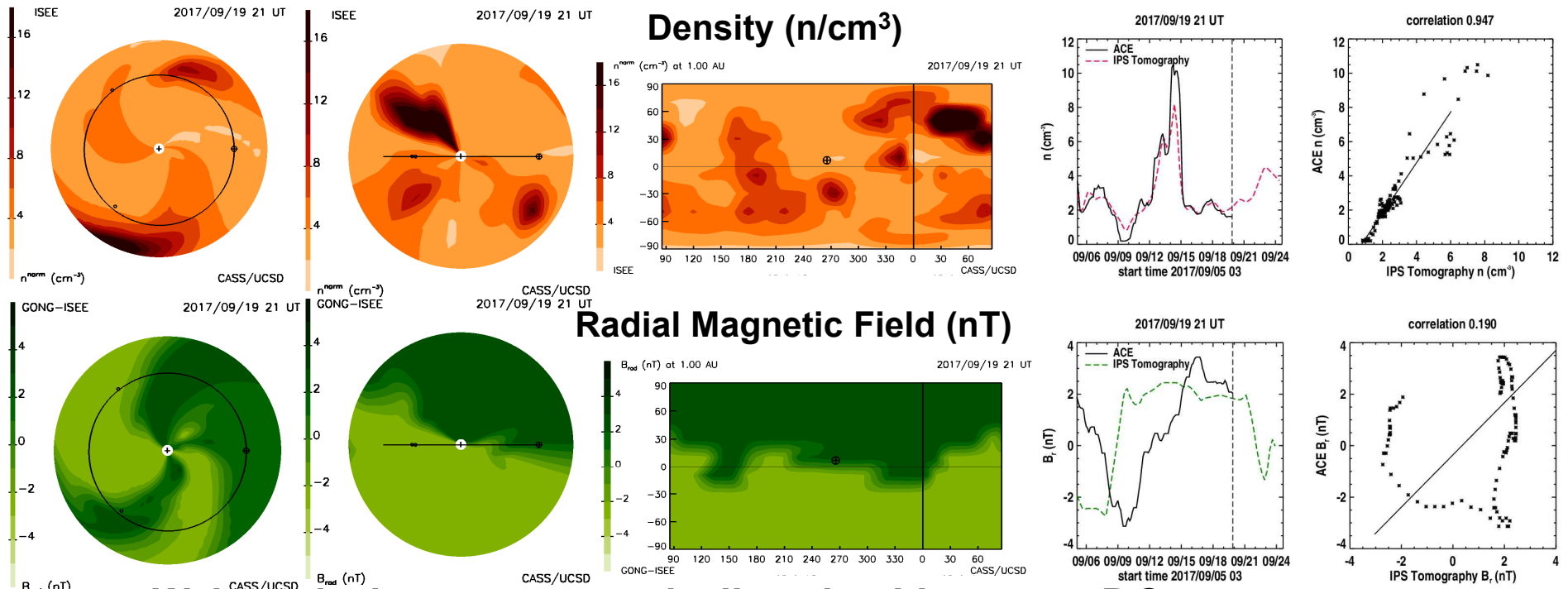
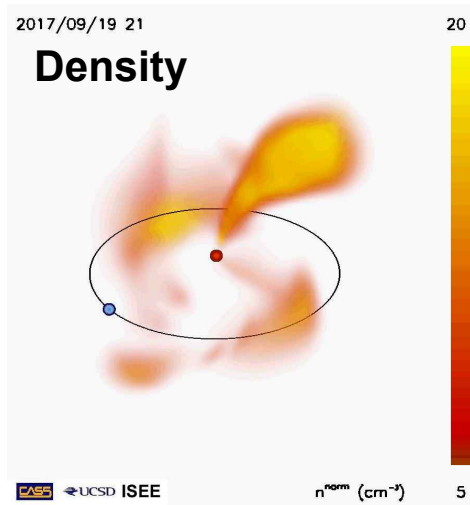
Web analysis runs “automatically” using Linux on a P.C.

Different Techniques for Measurement of Bz Heliospheric Remote Sensing

UCSD Prediction

(http://ips.ucsd.edu/high_resolution_predictions)

Today's 21 UT Analysis from ISEE



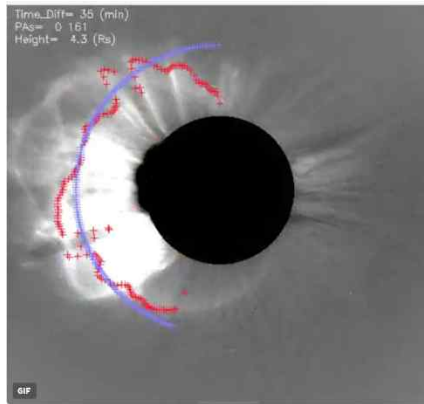
Web analysis runs automatically using Linux on a P.C.

Different Techniques for Measurement of Bz

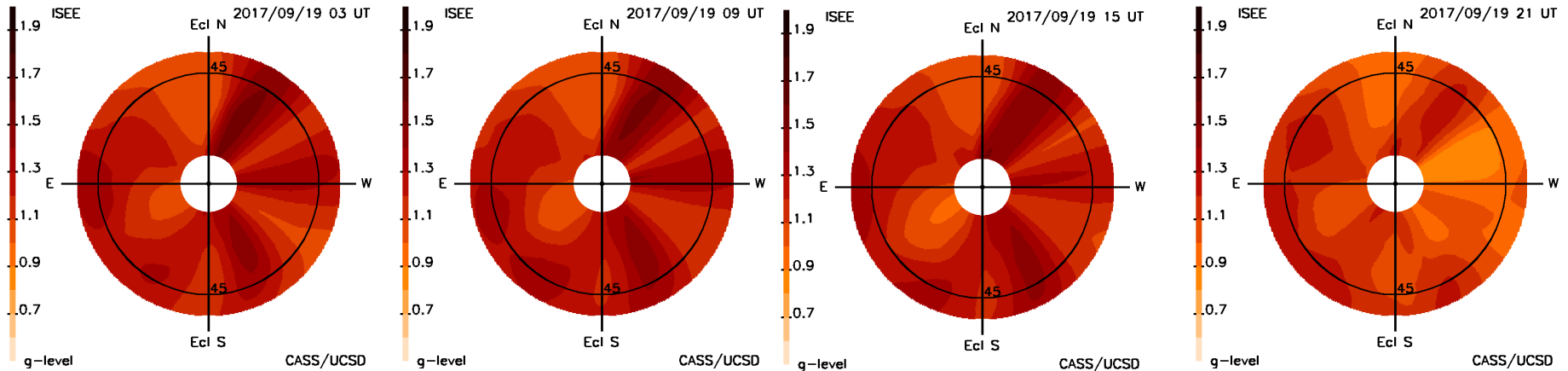
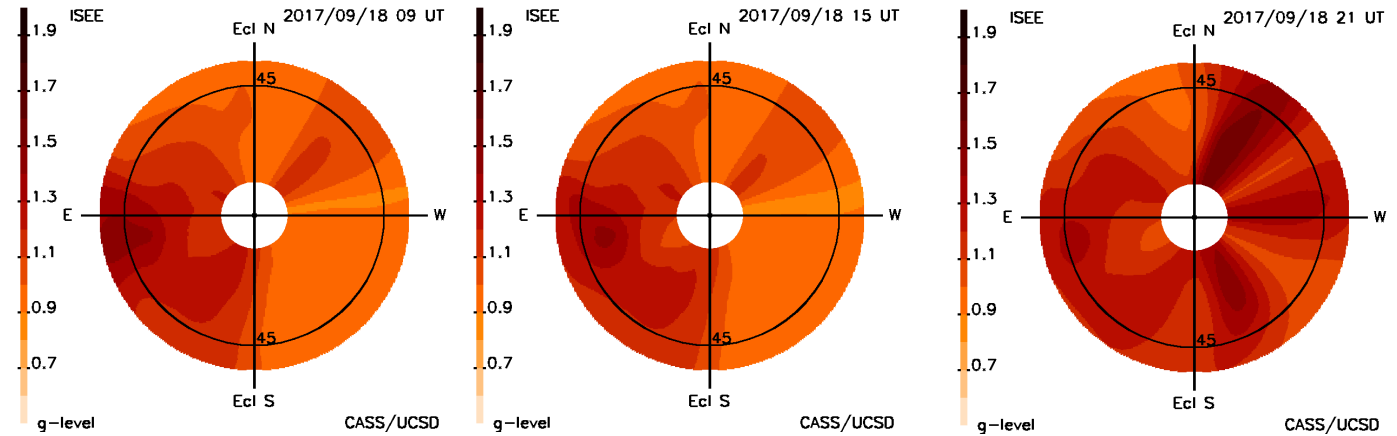
Heliospheric Remote Sensing

Backside halo CME sequence

2017/09/17 11:47 UT



11:47 AM - 17 Sep 2017



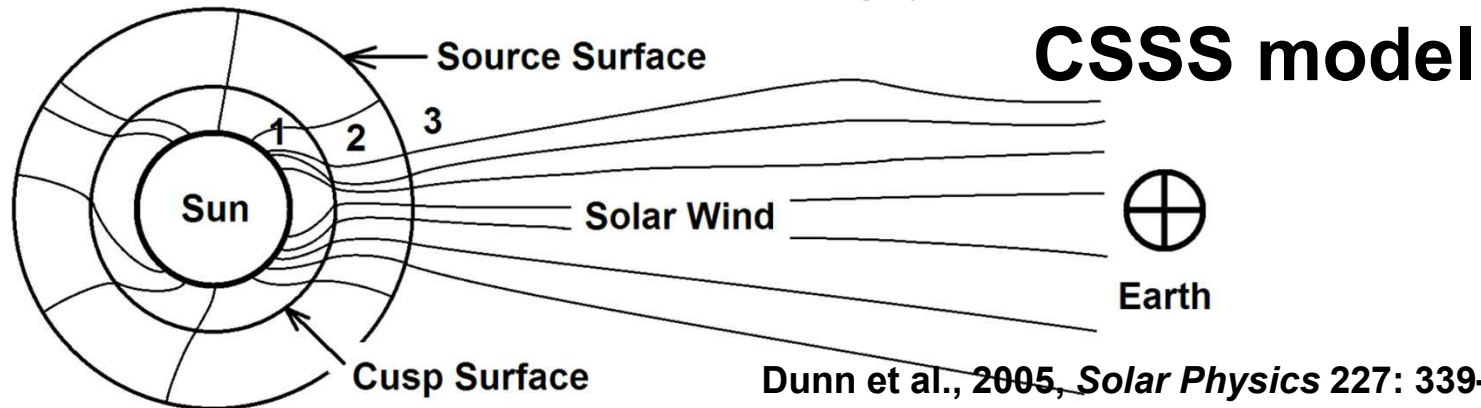
Different Techniques for Measurement of B_z

More Details

Magnetic Field

Different Techniques for Measurement of B_z Heliospheric Remote Sensing

(Zhao, X. P. and Hoeksema, J. T., 1995, *J. Geophys. Res.*, 100 (A1), 19.)

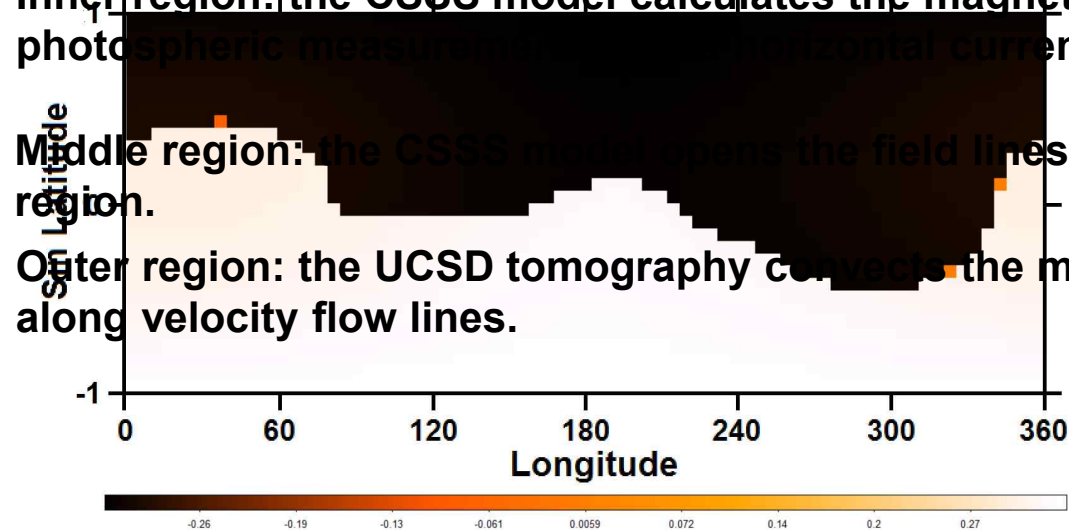


CSSS Model

UCSD Tomography

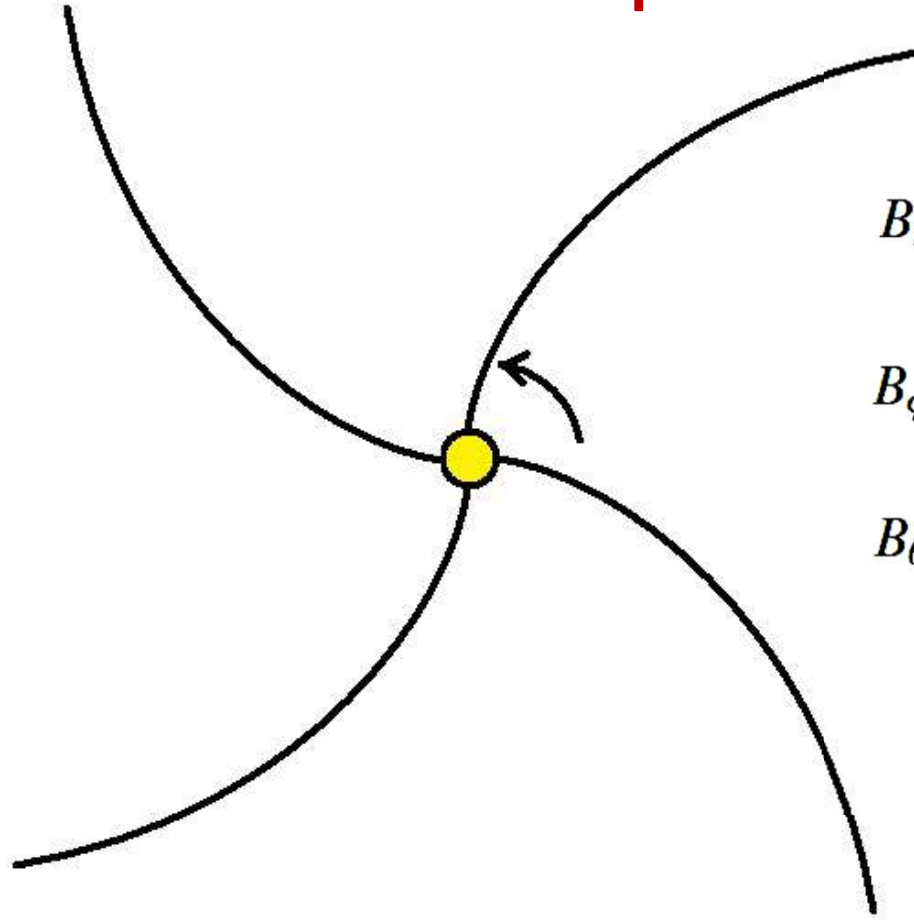
Source surface B_r field component sample

1. Inner region: the CSSS model calculates the magnetic field using photospheric measurements and a potential current model.
2. Middle region: the CSSS model follows the field lines. In the outer region.
3. Outer region: the UCSD tomography corrects the magnetic field along velocity flow lines.



Different Techniques for Measurement of Bz

Heliospheric Remote Sensing



$$B_r(r, \phi, \theta) = B(r_0, \phi_0, \theta_0) \left(\frac{r_0}{r} \right)^2$$

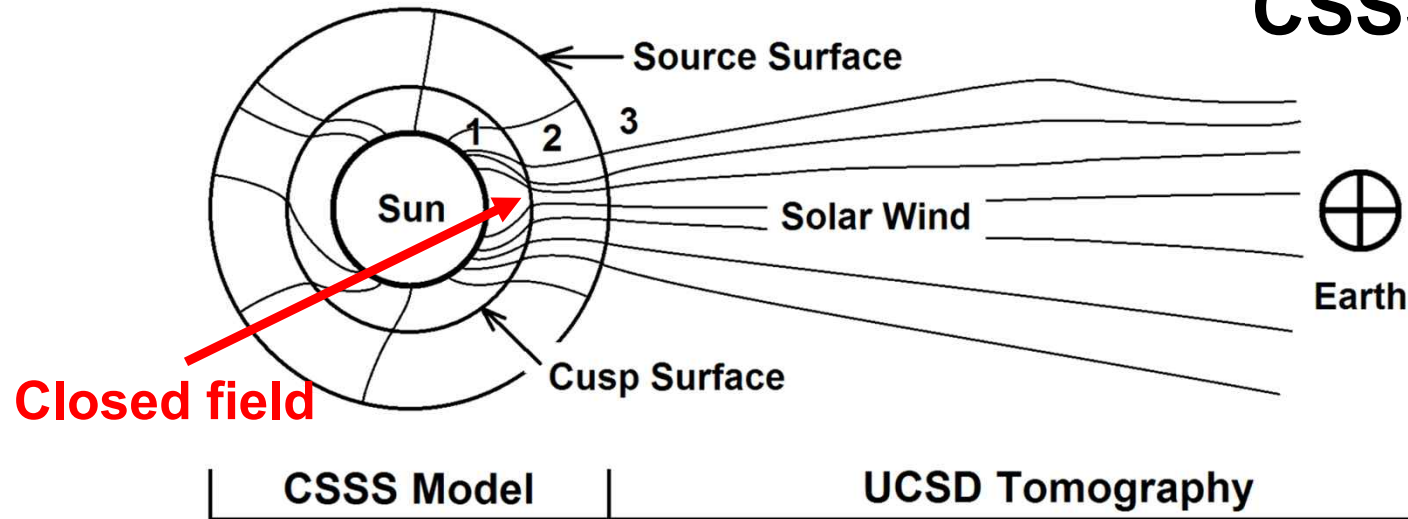
$$B_\phi(r, \phi, \theta) = -B(r) \left(\frac{\omega r_0 \sin(\theta)}{V} \right) \left(\frac{r_0}{r} \right)$$

$$B_\theta(r, \phi, \theta) = 0$$

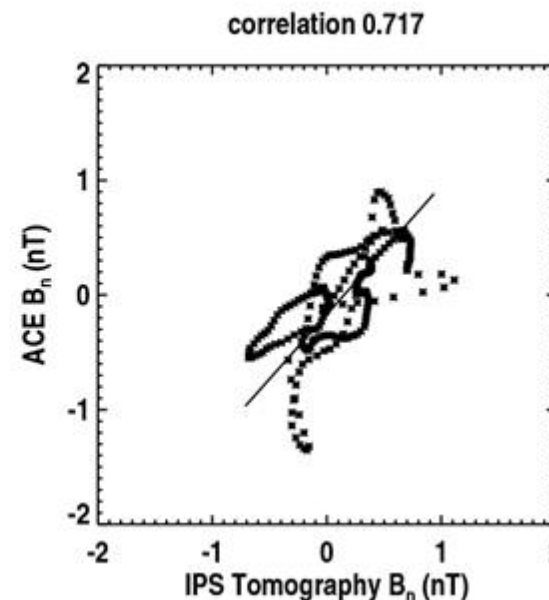
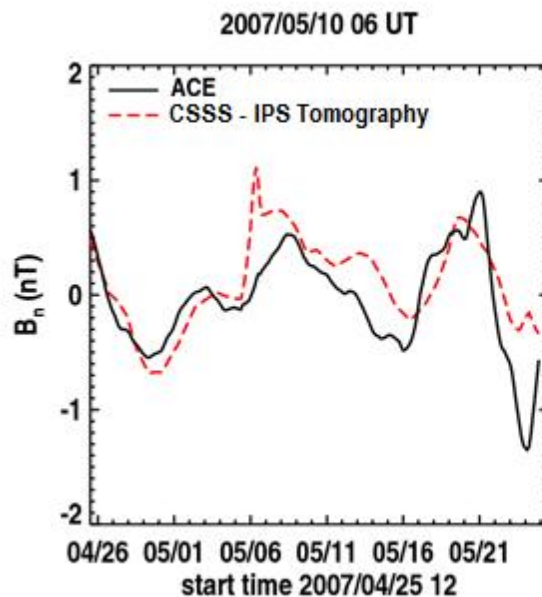
Different Techniques for Measurement of Bz

(Jackson, B.V., et al., 2015, *ApJL*, 803:L1. 1- 5, doi:10.1088/2041-8205/803/1/L1.)

CSSS model



Extrapolated B_n closed field component for CR 2056

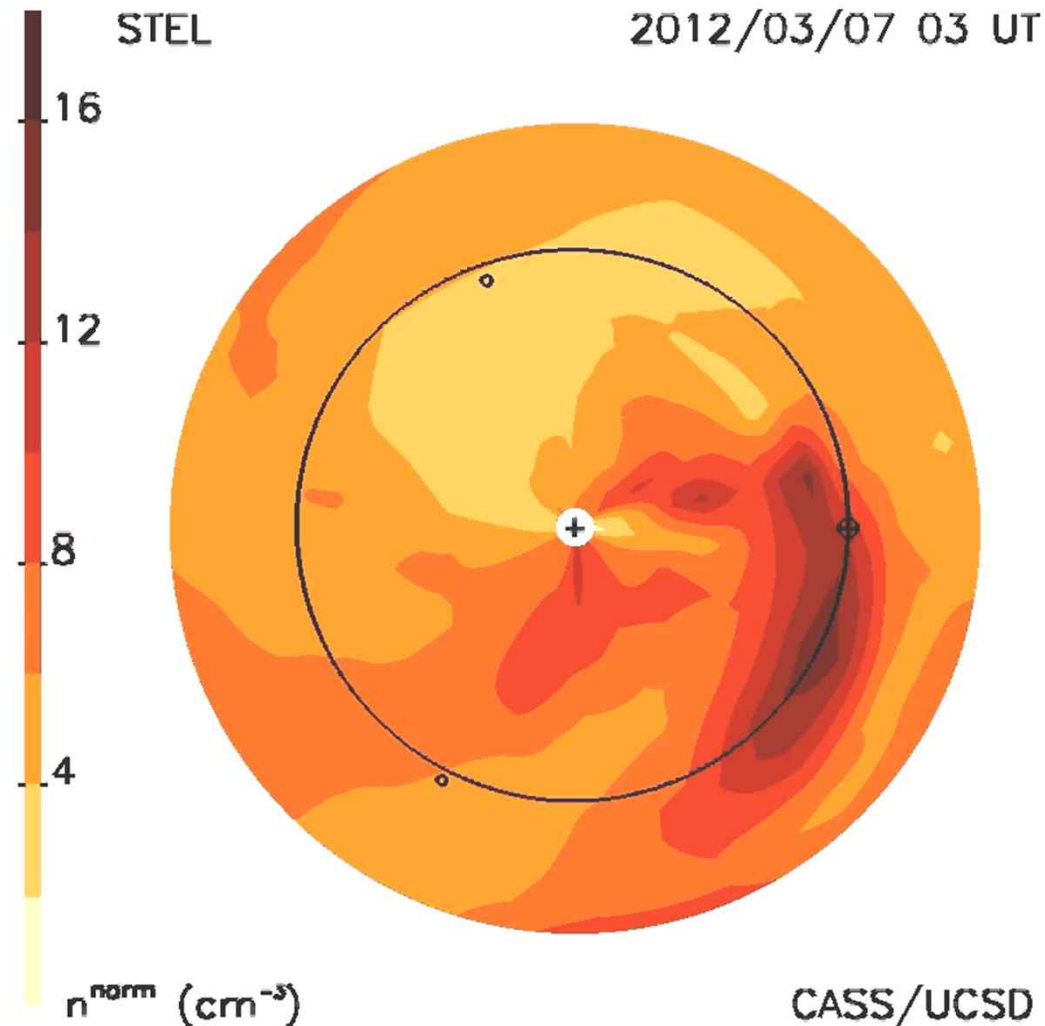


About
1/50th of
the static
flux $r^{-1.34}$
fall-off

Different Techniques for Measurement of Bz

Heliospheric Remote Sensing

$$\Phi = \lambda^2 \int n_e \bar{\mathbf{B}} \cdot d\bar{\mathbf{s}}$$

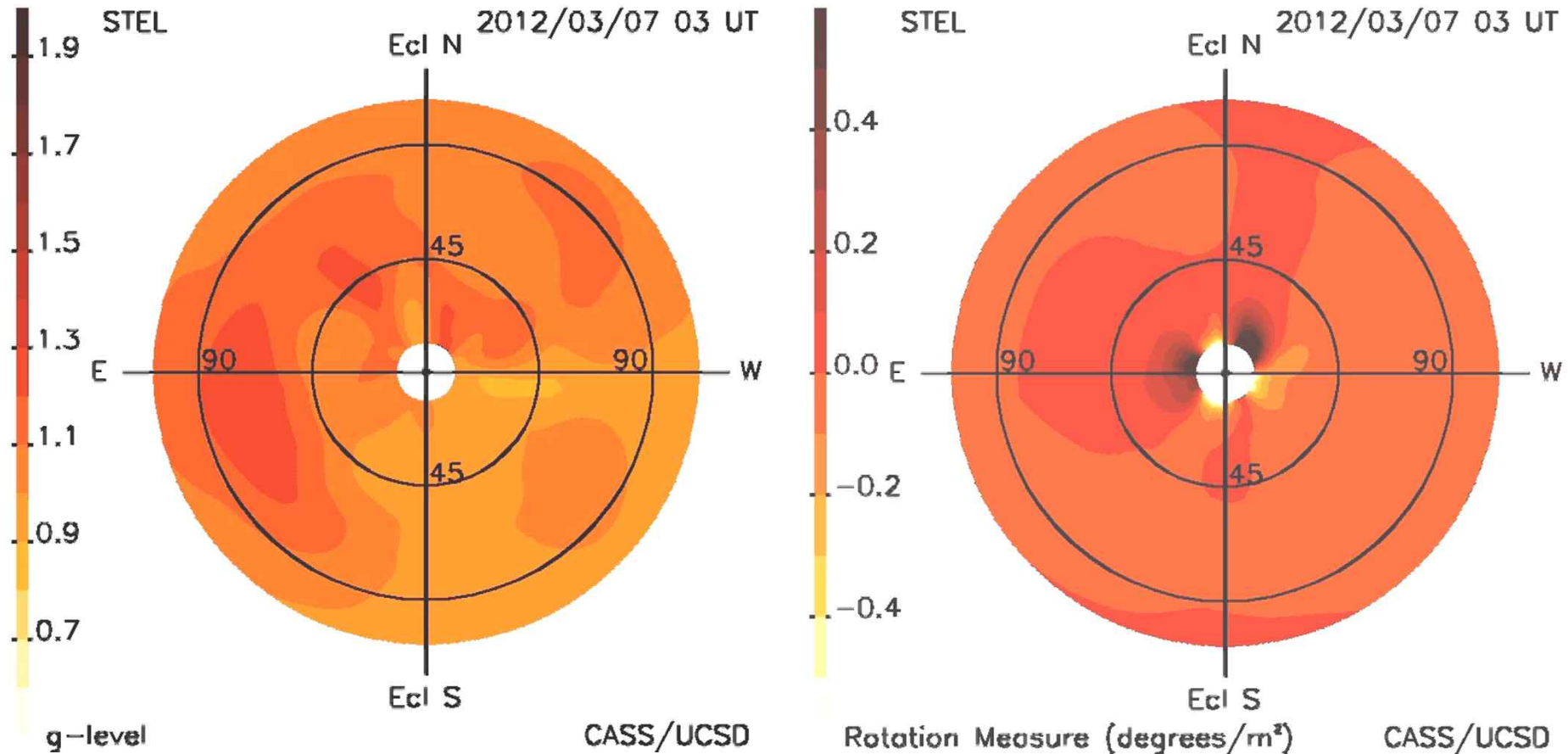


3-D reconstructions of Carrington rotation (CR) 2121 showing a CME of interest from 07 March 2012 launched around 01:00UT.

Different Techniques for Measurement of Bz

Heliospheric Remote Sensing

$$\Phi = \lambda^2 \int n_e \bar{\mathbf{B}} \cdot \bar{\mathbf{d}}s$$



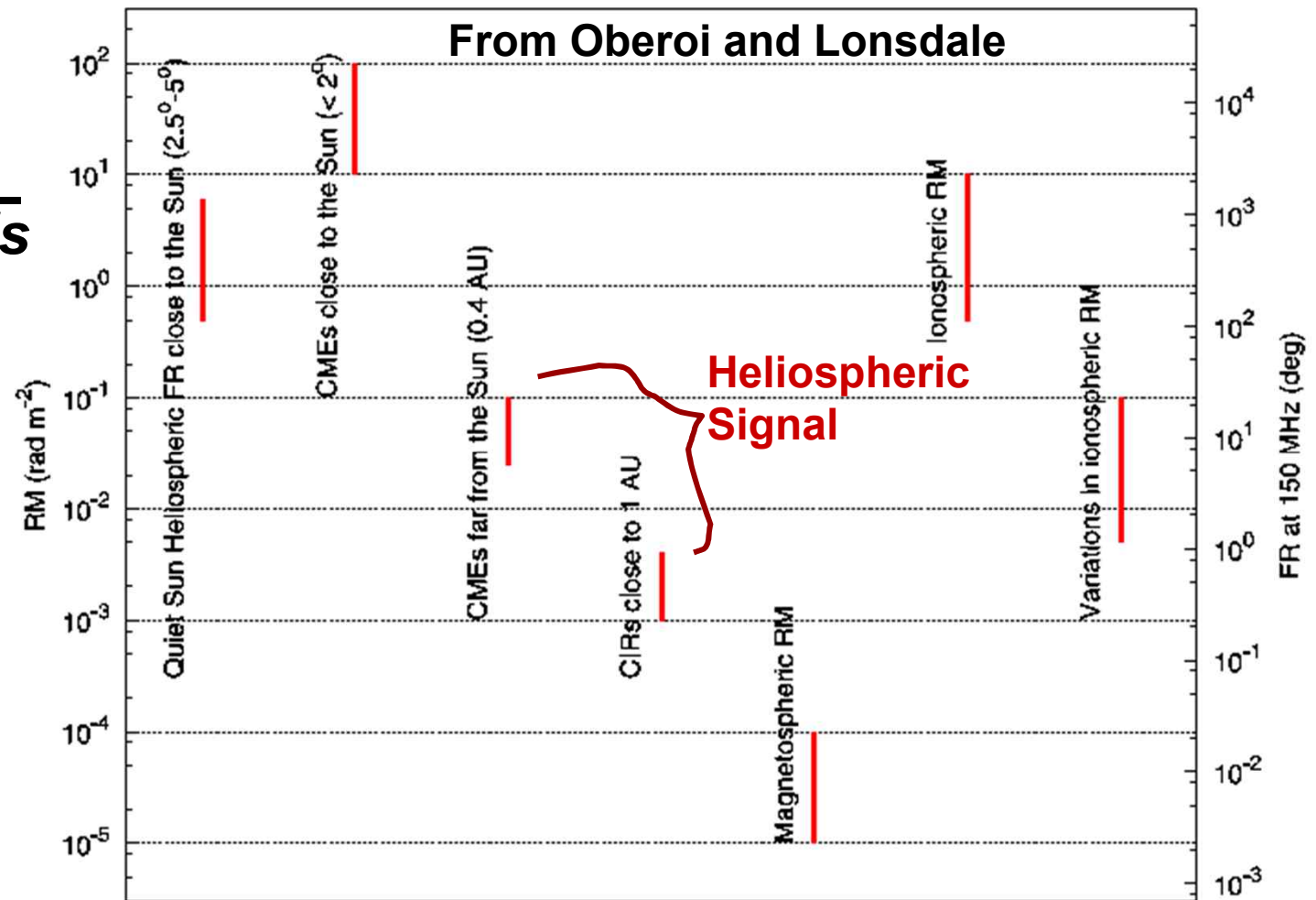
The same period extracted from CR2121 comparing IPS *g*-level fish-eye sky map (left) with that of reconstructed RM from ambient magnetic fields (right) perturbed by the CME.

Different Techniques for Measurement of Bz Heliospheric Remote Sensing

Oberoi and Lonsdale, 2012, *Radio Science*, 47, RS0K08, doi:10.1029/2012RS004992.

Faraday rotation signals at low frequency

$$\Phi = \lambda^2 \int n_e \bar{B} \cdot d\bar{s}$$



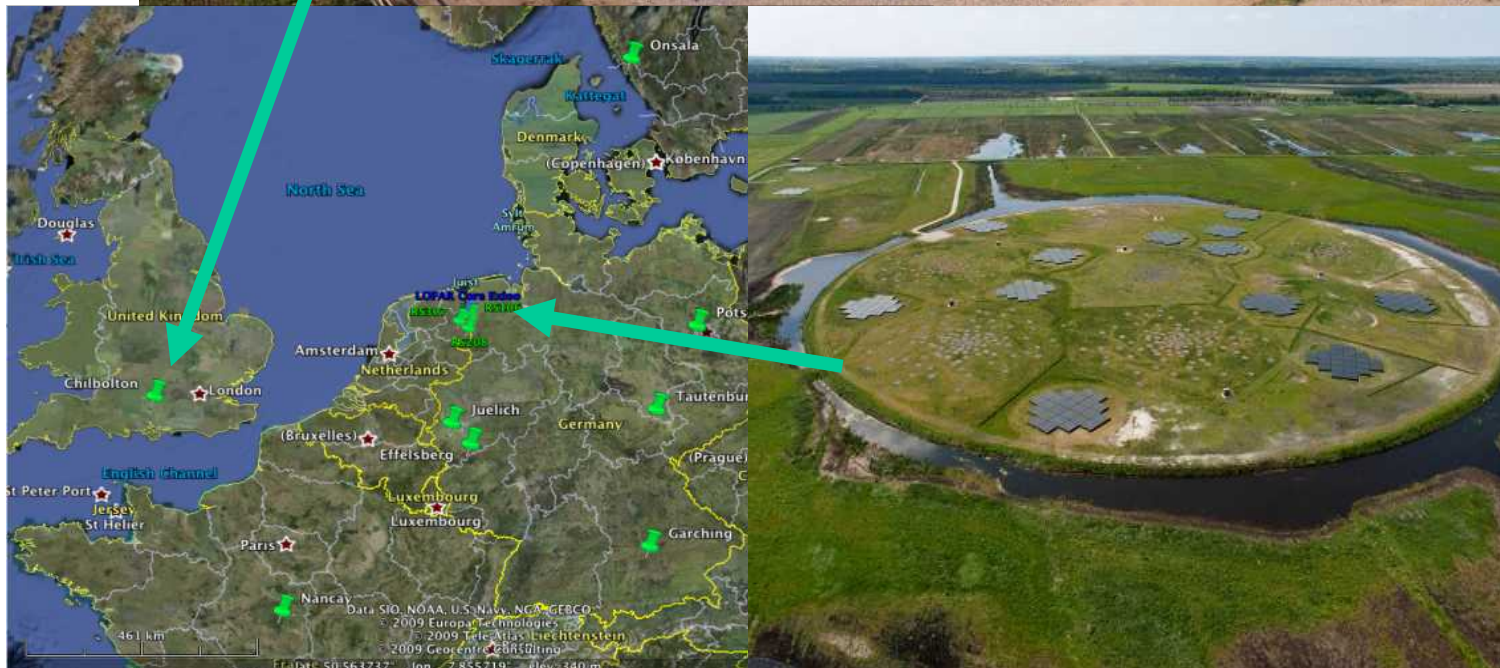
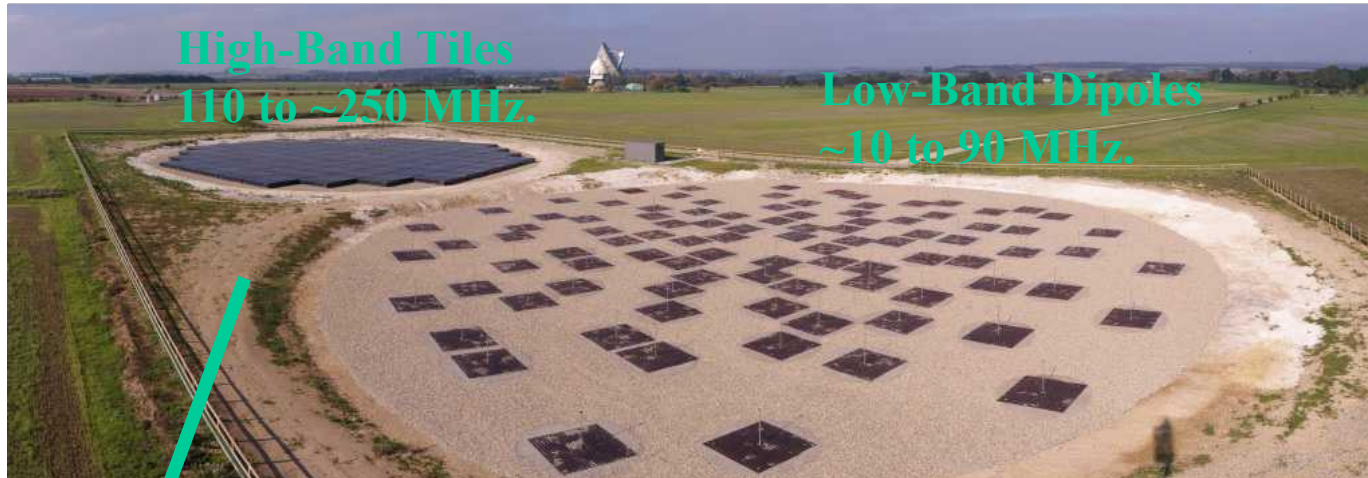
Different Techniques for Measurement of Bz

Heliospheric Remote Sensing

Fm Mario Bisi

LOFAR

ASTRON

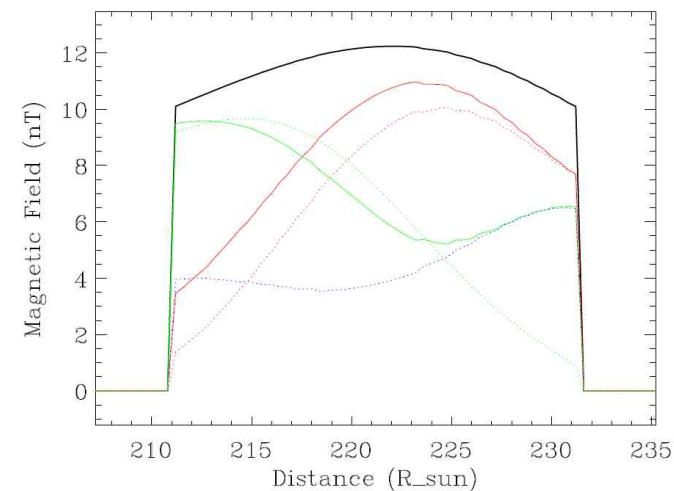
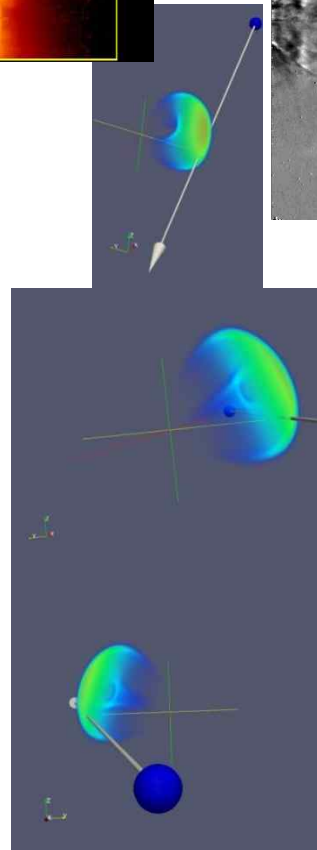
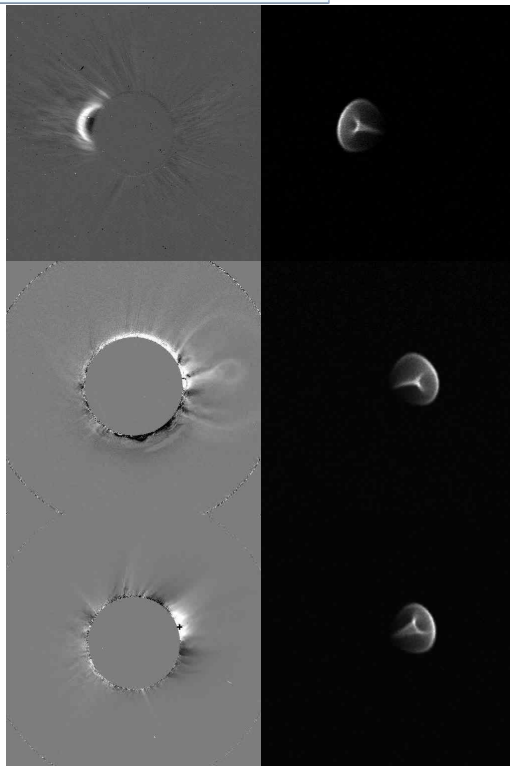
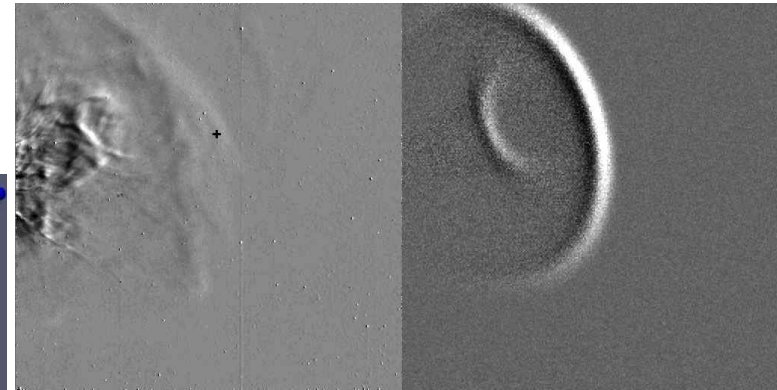
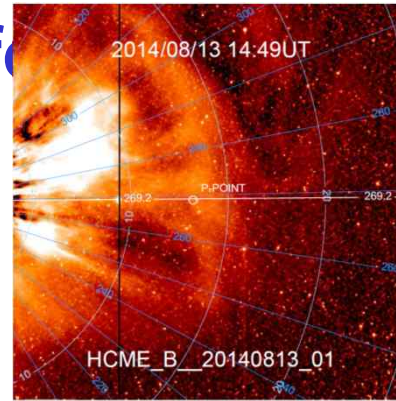
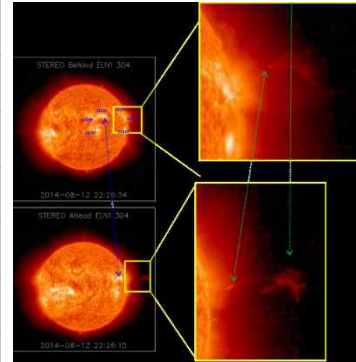
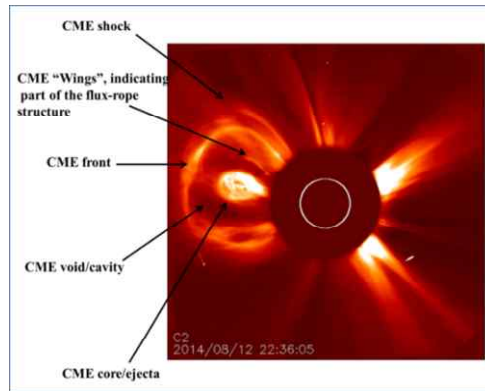


Different Techniques for the Measurement of Bz

Fm Mario Bisi

© 2017 RAL Space

Heliospheric FR Observation



Different Techniques for Measurement of Bz

Heliospheric Remote Sensing

© 2017 RAL Space

Fm Mario Bisi

Heliospheric FR Observations (3)

Time	Observed RM	Ion RM	Total RM
13:00	3.12722 ± 0.02	2.48140 ± 0.12264	0.64582 ± 0.12426
13:20	2.72809 ± 0.02	2.56207 ± 0.13366	0.16602 ± 0.13515
13:40	2.97102 ± 0.02	2.49809 ± 0.12492	0.47293 ± 0.10598
14:00	$3.06306 \pm \text{—}$	2.48251 ± 0.14120	$0.58055 \pm \text{—}$
14:20	$3.10321 \pm \text{—}$	2.46633 ± 0.12987	$0.63688 \pm \text{—}$
14:40	3.12737 ± 0.04	2.47916 ± 0.13886	0.64821 ± 0.14451
15:00	2.99077 ± 0.02	2.37482 ± 0.11960	0.61595 ± 0.12126

- Using simple dimensional-analysis calculations:

$RM = 0.002 \times ne[\text{cm}^{-3}] \times B[\text{nT}] \times L[\text{AU}]^\circ \text{ m}^{-2}$, where L is the contributing integration length along the LOS, we get a maximum expected RM value: $RM = 0.002 \times 669 \times 150 \times 0.25 = 50.2^\circ \text{ m}^{-2}$ (or 0.928 rad m^{-2}); perhaps high – but is very much in line with the LOFAR preliminary heliospheric RM values.

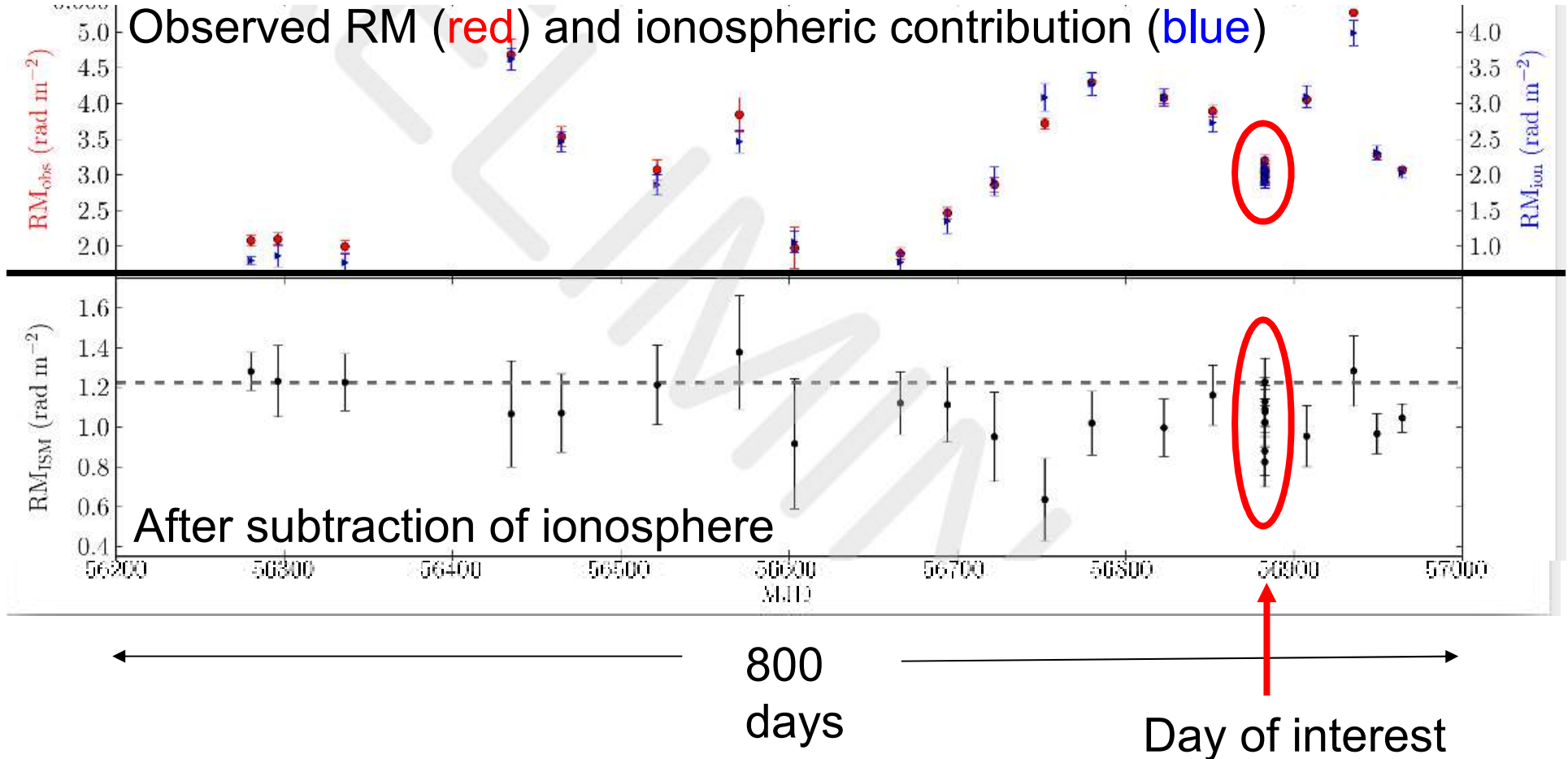
Different Techniques for Measurement of Bz

Heliospheric Remote Sensing

Interstellar Medium Variations

Fm Richard Fallows

Plot courtesy Charlotte Sobey, CSIRO

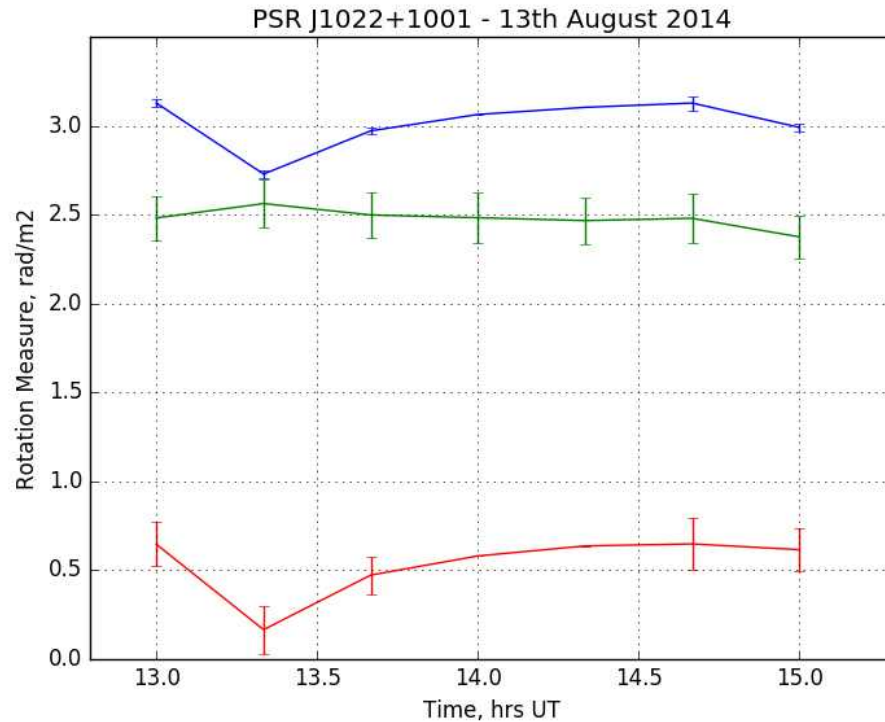


Different Techniques for Measurement of Bz

Fm Richard Fallows

Heliospheric Remote Sensing

RM Calculations – Current Estimates



Measured RM (ISM subtracted)

Calculated Ionospheric RM

RM difference

Modelling and number checking efforts underway indicate that the resulting difference in RM, assumed to be due to the heliosphere, is in the ballpark for that expected from the passage of this CME.

Different Techniques for Measurement of Bz

In the meantime

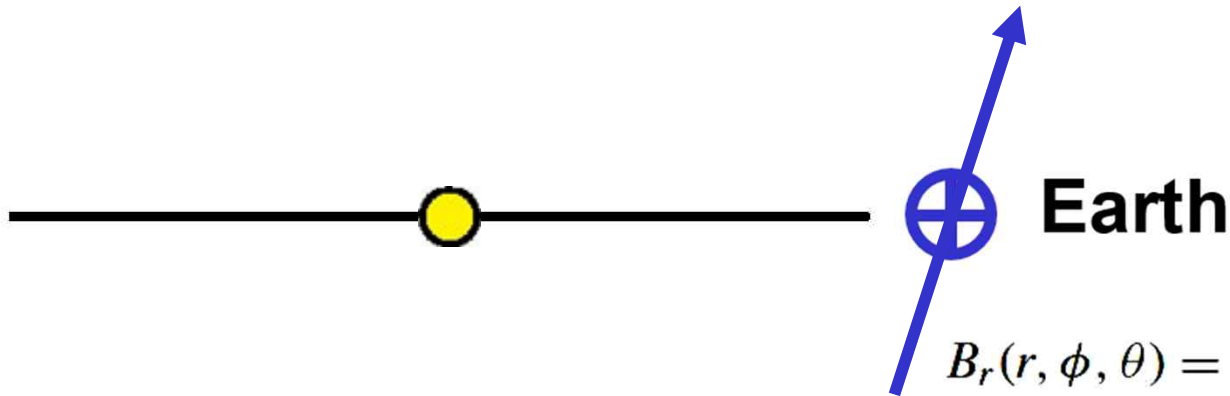
Choi *et al.*, JGR, 122, 4921, doi: 10.1002/2016JA023836

“...for substorms of weak to medium...even the weakly (in terms of either intensity or duration) southward IMF Bz should be considered significant...”

Magnetic Field
Russell - McPherron Effect
“Daily Implementation”

Different Techniques for Measurement of Bz GSM coordinates

(Russell, C. T., and McPherron, R. L., 1973, *J. Geophys. Res.*, 78 (1), 92.)



$$B_r(r, \phi, \theta) = B(r_0, \phi_0, \theta_0) \left(\frac{r_0}{r} \right)^2$$

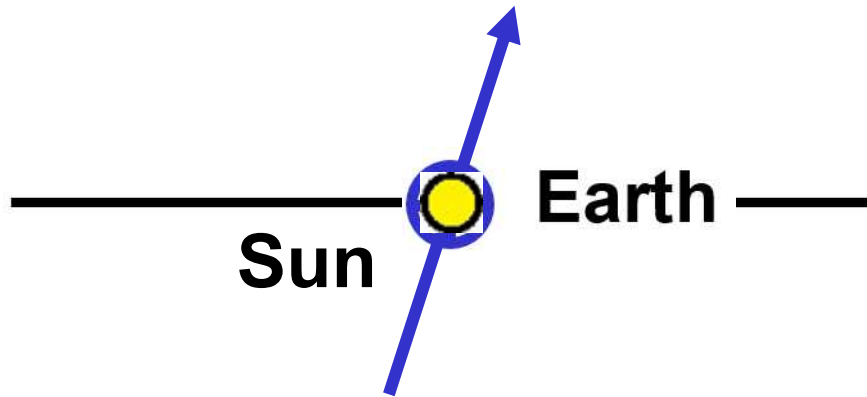
$$B_\phi(r, \phi, \theta) = -B(r) \left(\frac{\omega r_0 \sin(\theta)}{V} \right) \left(\frac{r_0}{r} \right)$$

$$B_\theta(r, \phi, \theta) = 0$$

Different Techniques for Measurement of Bz

GSM coordinates

(Russell, C. T., and McPherron, R. L., 1973, *J. Geophys. Res.*, 78 (1), 92.)



$$B_r(r, \phi, \theta) = B(r_0, \phi_0, \theta_0) \left(\frac{r_0}{r} \right)^2$$

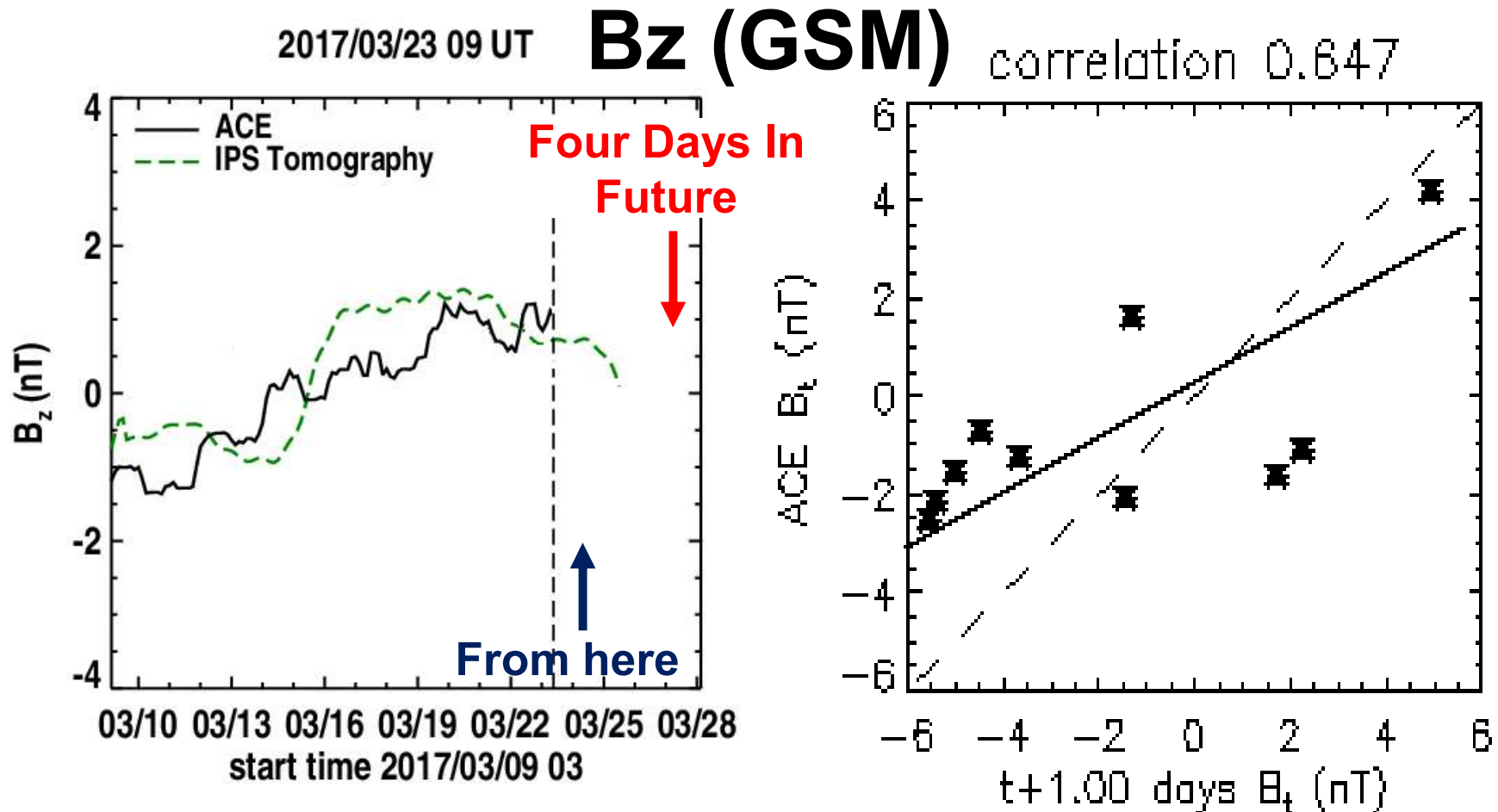
$$B_\phi(r, \phi, \theta) = -B(r) \left(\frac{\omega r_0 \sin(\theta)}{V} \right) \left(\frac{r_0}{r} \right)$$

$$B_\theta(r, \phi, \theta) = 0$$

Different Techniques for Measurement of Bz

(see: http://ips.ucsd.edu/ips_workshop_2016)

UCSD Prediction Analyses Last March Analyses from ISEE: Day -4

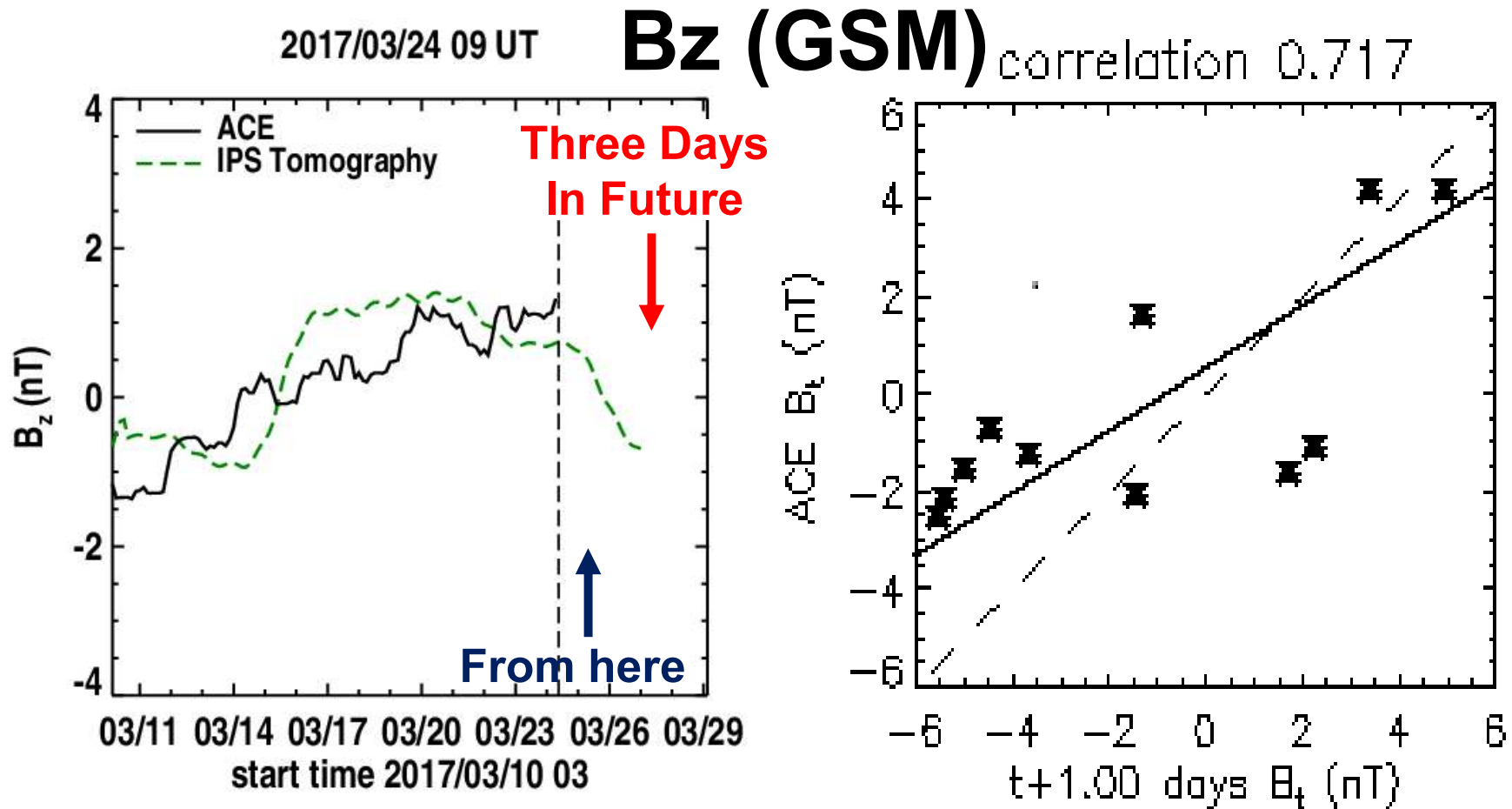


Web analysis runs automatically using Linux on a P.C.

Different Techniques for Measurement of Bz

(see: http://ips.ucsd.edu/ips_workshop_2016)

UCSD Prediction Analyses Last March Analyses from ISEE: Day -3

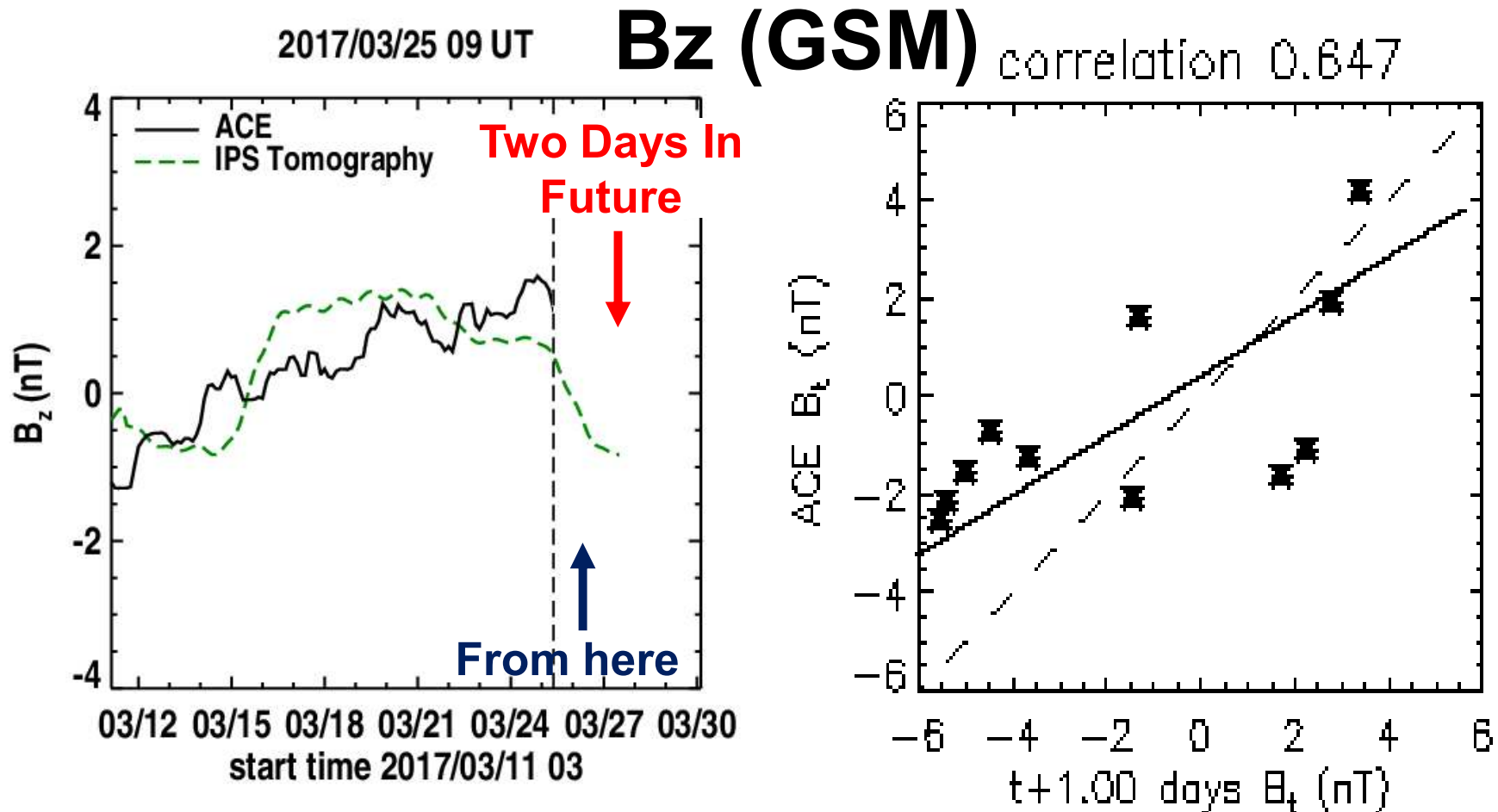


Web analysis runs automatically using Linux on a P.C.

Different Techniques for Measurement of Bz

(see: http://ips.ucsd.edu/ips_workshop_2016)

UCSD Prediction Analyses Last March Analyses from ISEE: Day -2

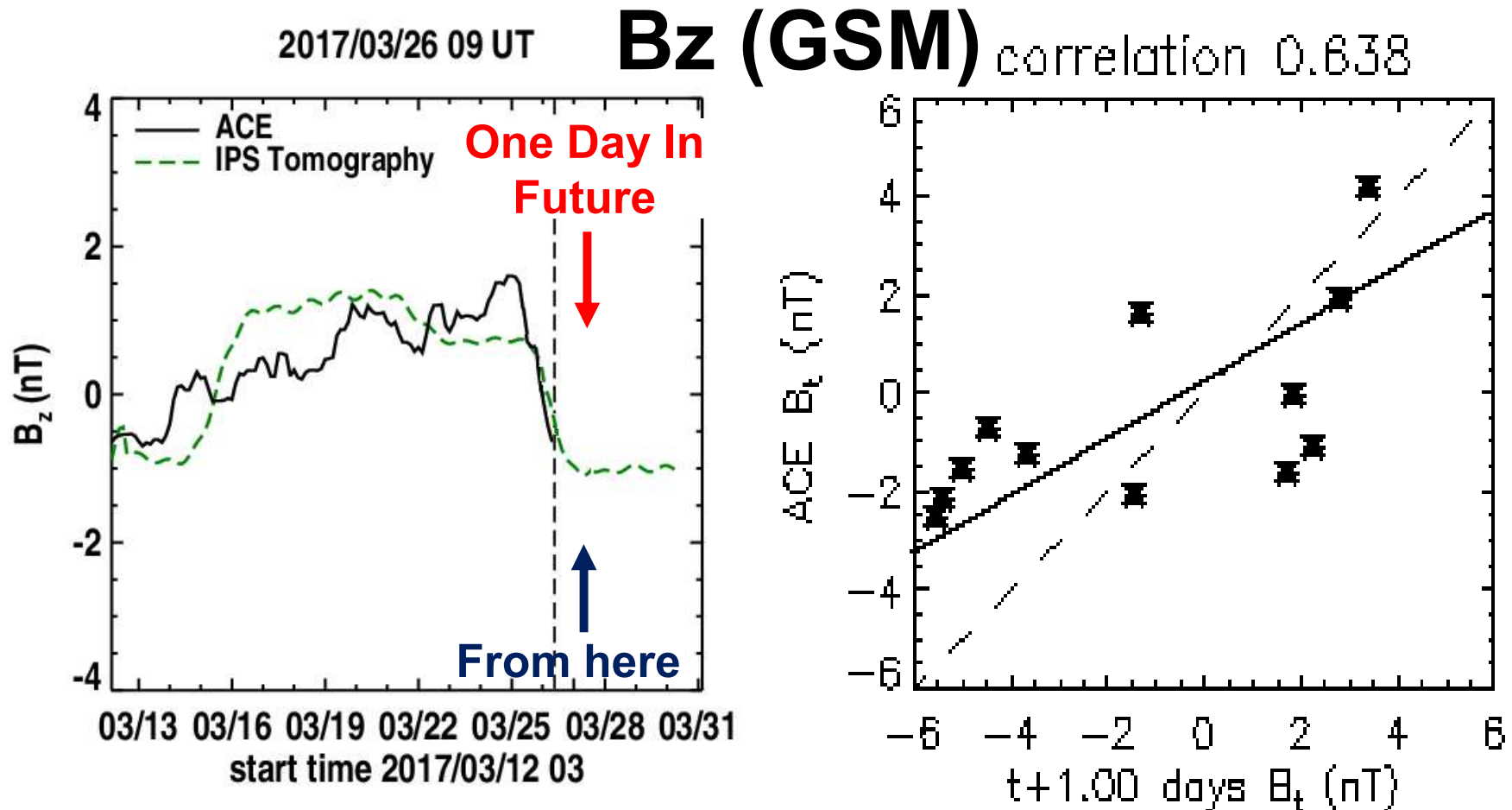


Web analysis runs automatically using Linux on a P.C.

Different Techniques for Measurement of Bz

(see: http://ips.ucsd.edu/ips_workshop_2016)

UCSD Prediction Analyses Last March Analyses from ISEE: Day -1

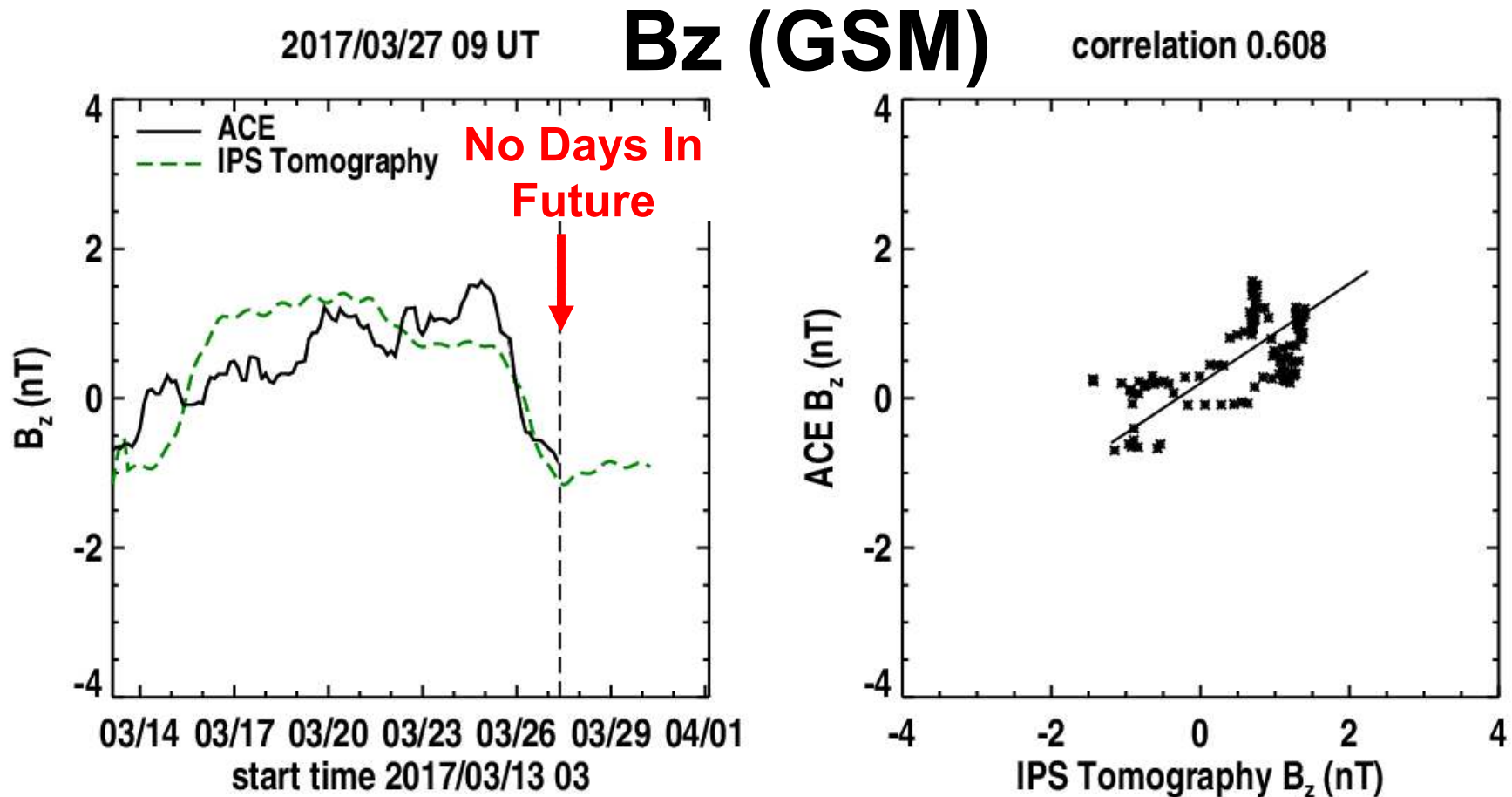


Web analysis runs automatically using Linux on a P.C.

Different Techniques for Measurement of B_z

(see: http://ips.ucsd.edu/ips_workshop_2016)

UCSD Prediction Analyses Last March Analyses from ISEE: Day -1



Web analysis runs automatically using Linux on a P.C.

Different Techniques for Measurement of Bz

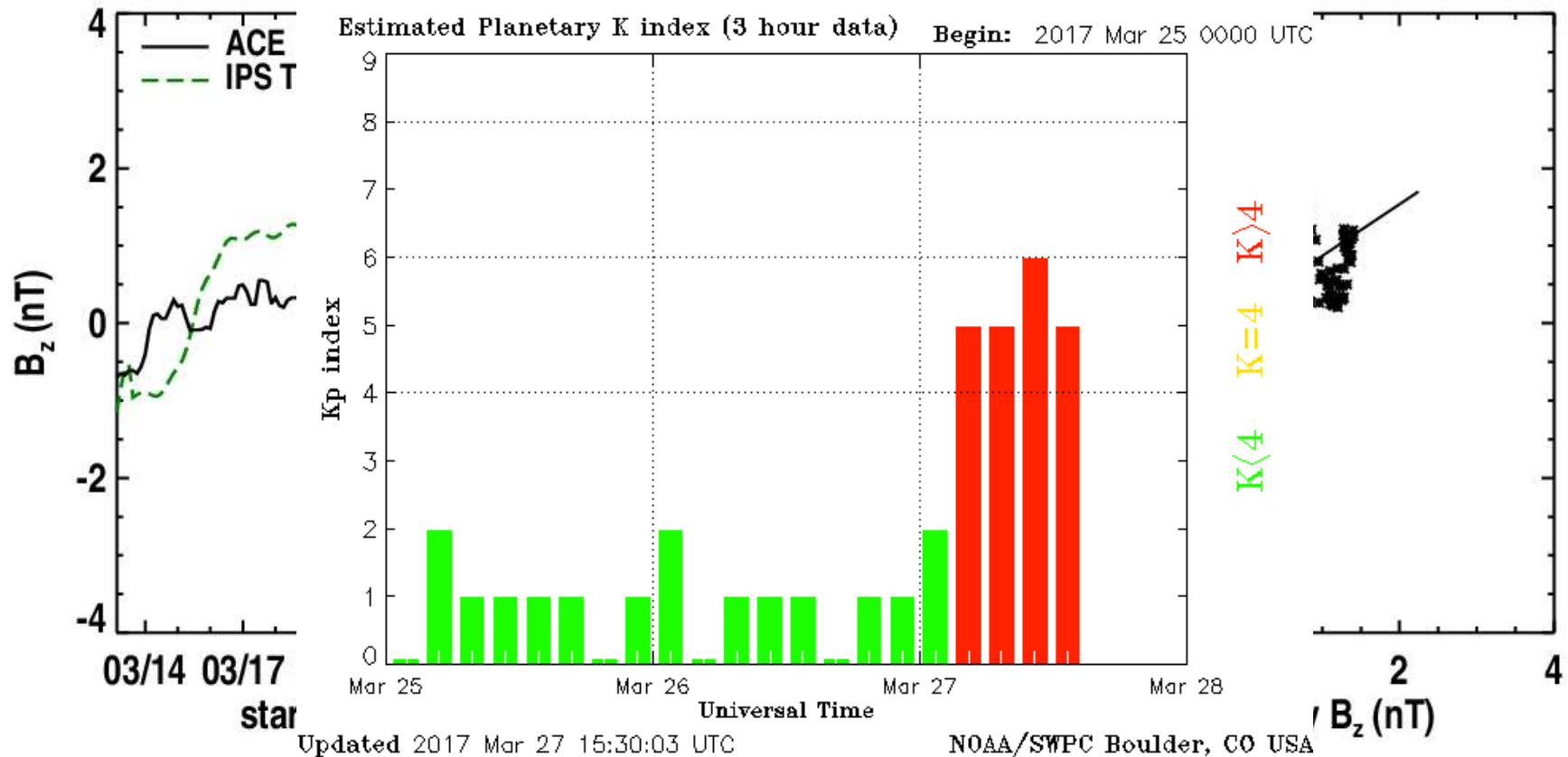
(see: http://ips.ucsd.edu/ips_workshop_2016)

UCSD Predictions Magnetic Field Analysis

2017/03/27 09 UT

NOAA Kp

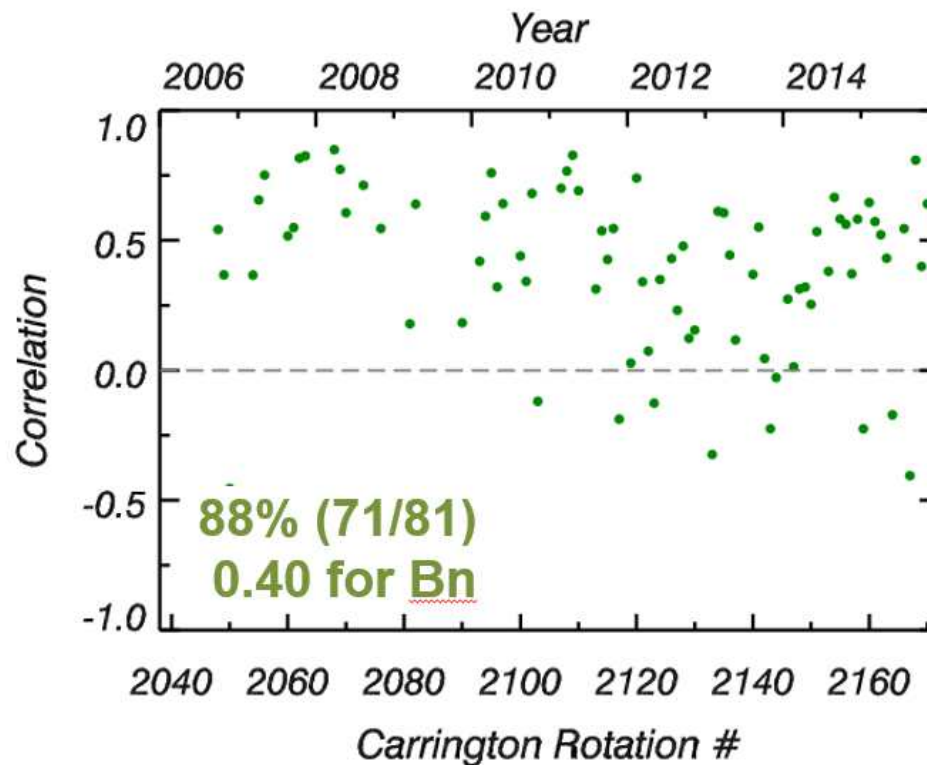
correlation 0.608



Web analysis runs automatically using Linux on a P.C.

Different Techniques for Measurement of Bz

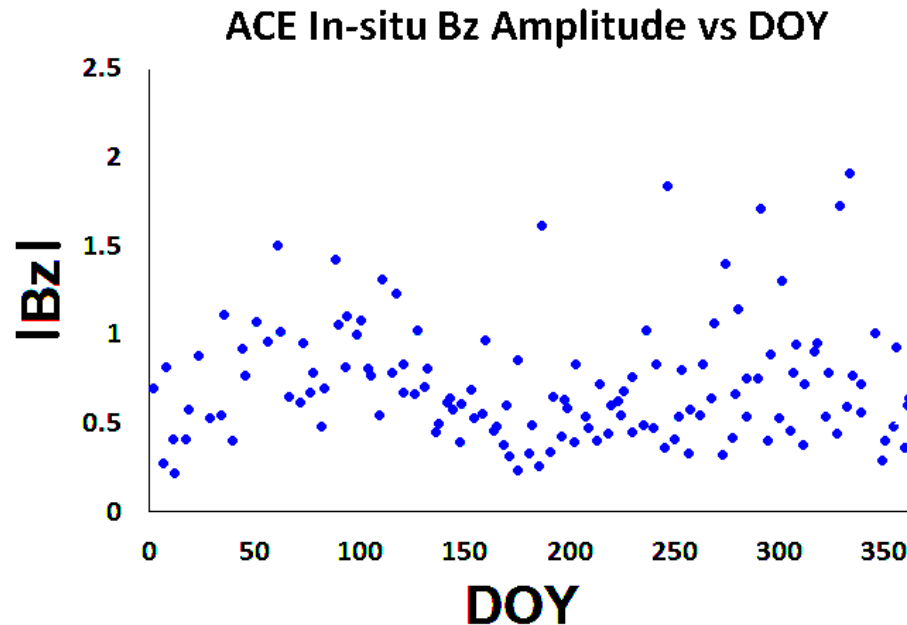
ACE and IPS-derived Bz Pearson's R Correlation per Carrington Rotation in GSM Coordinates over Ten Years



← Positive Correlations
(over 10 years)

(CRs of Bz excursion < 0.25 nT
are removed)

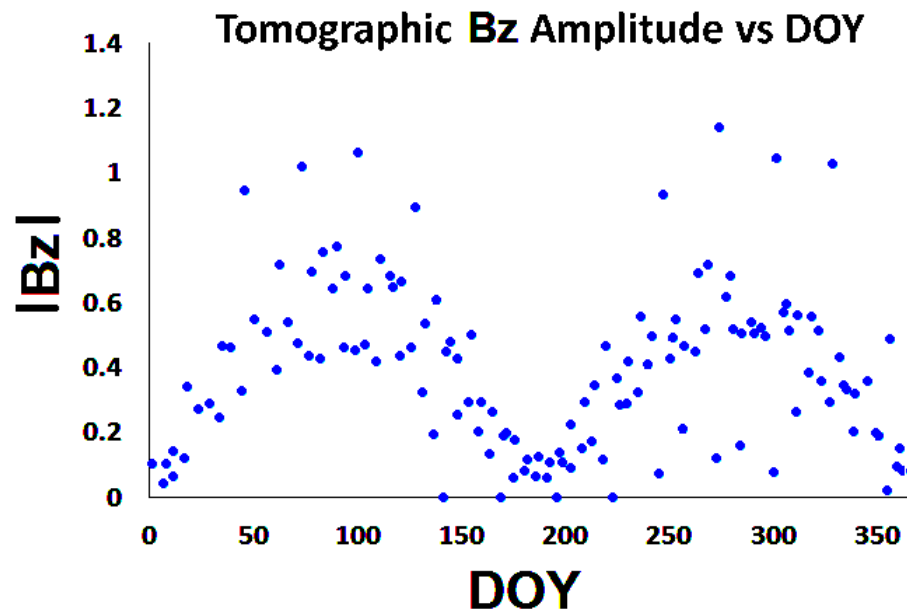
Different Techniques for Measurement of Bz



(Russell, C. T., and McPherron, R. L.,
1973, *J. Geophys. Res.*, 78 (1), 92.)

**10 years of
ACE data**

**Bz Amplitude
in GSM
coordinates**

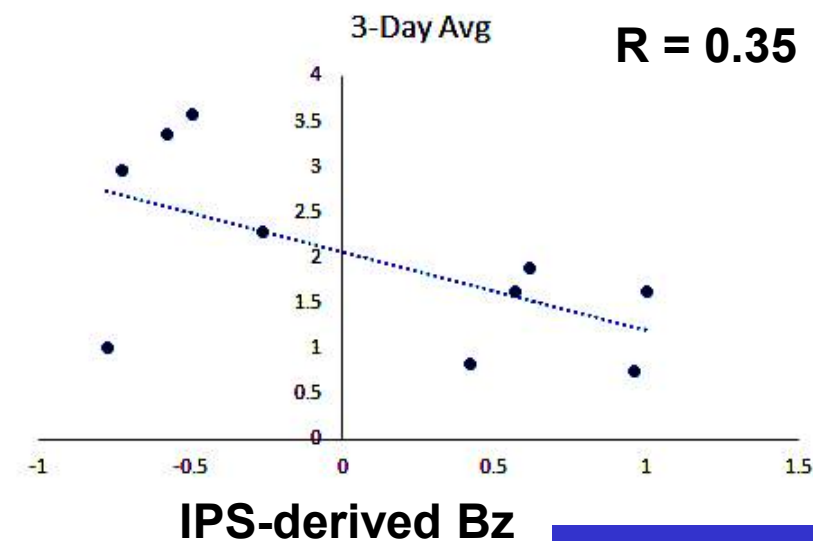
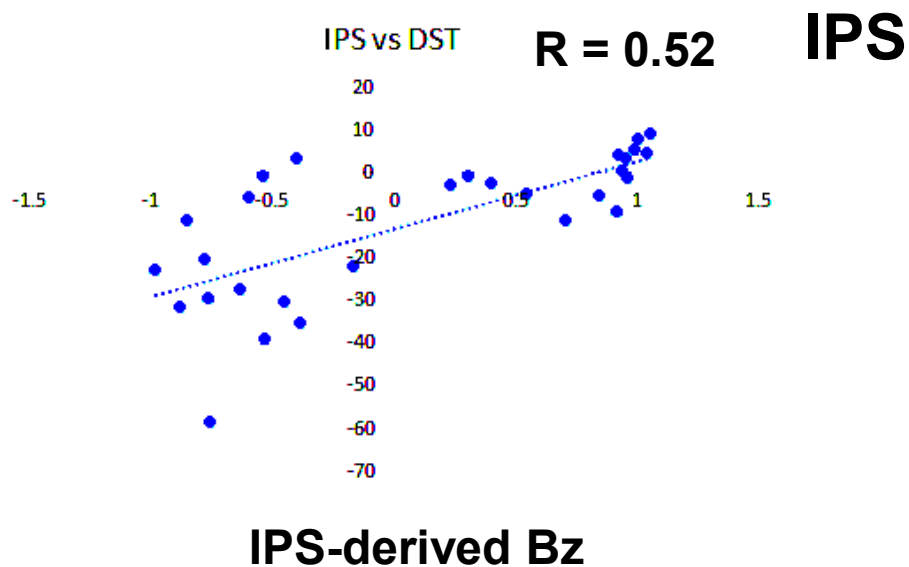
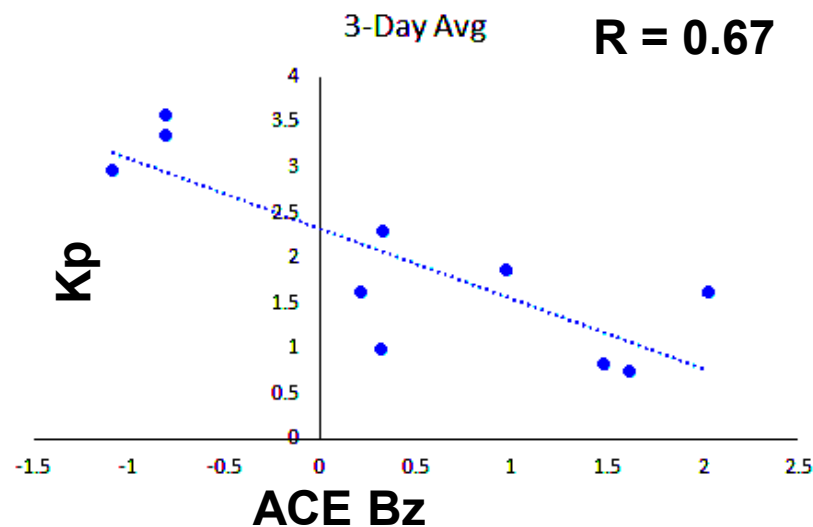
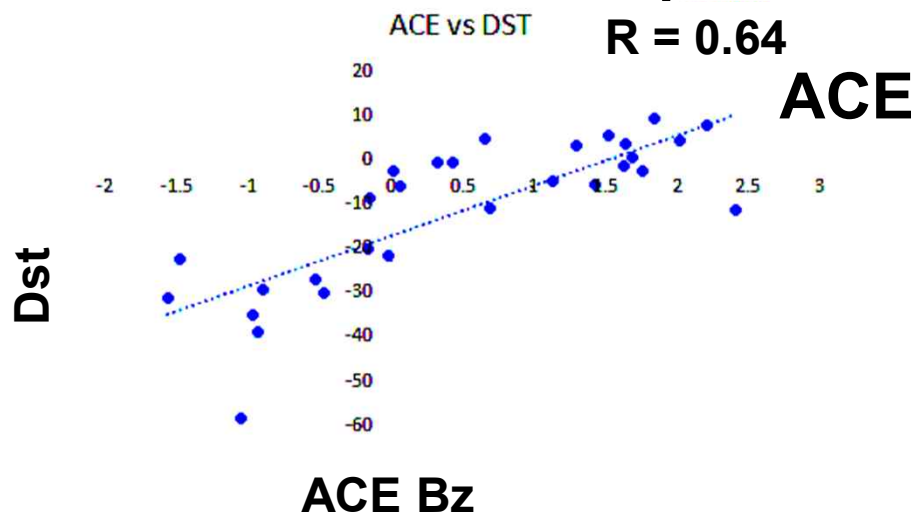


**10 years of
GONG data –
IPS extrapolation**

Different Techniques for Measurement of Bz

UCSD Prediction Analyses - 2016 Study

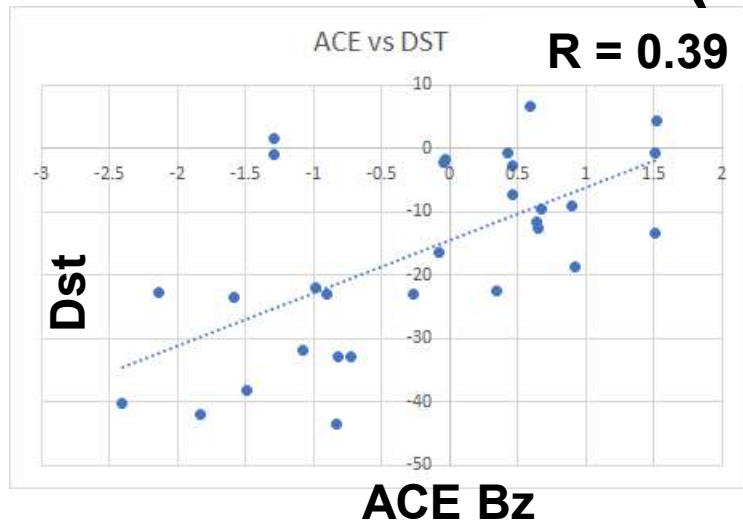
Dst vs GSM Bz (CR 2074) Kp vs GSM Bz



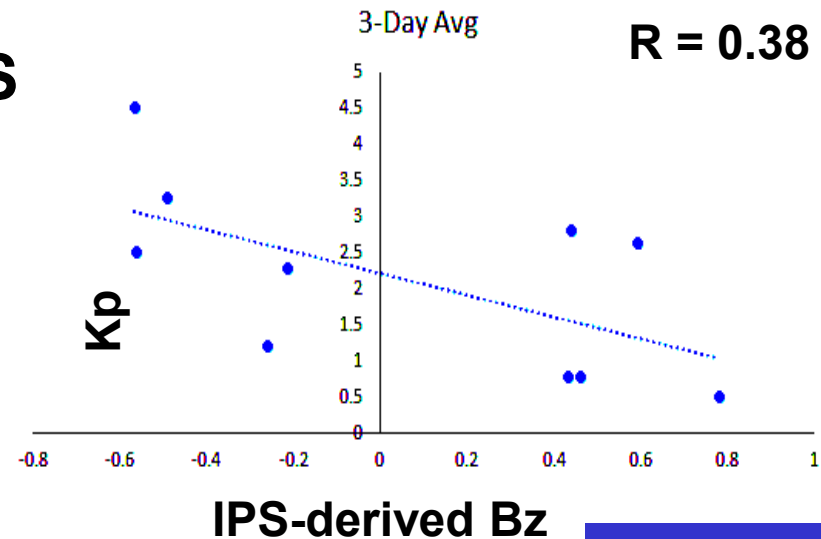
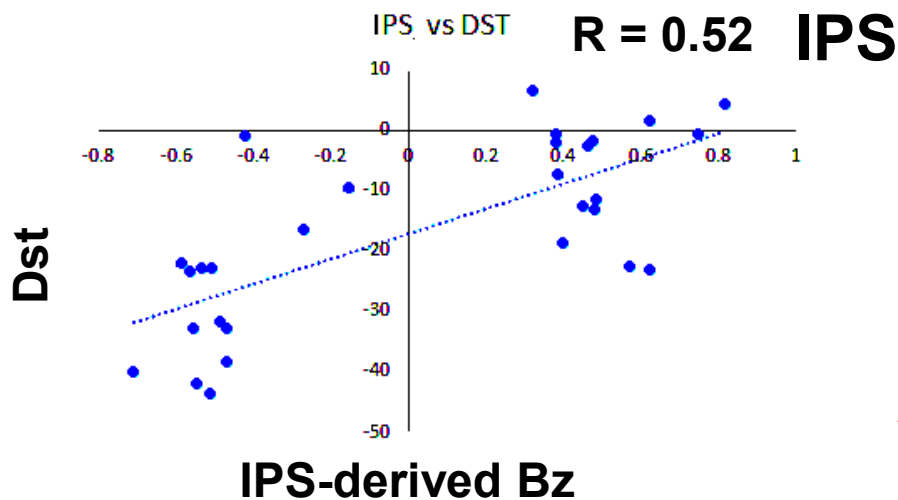
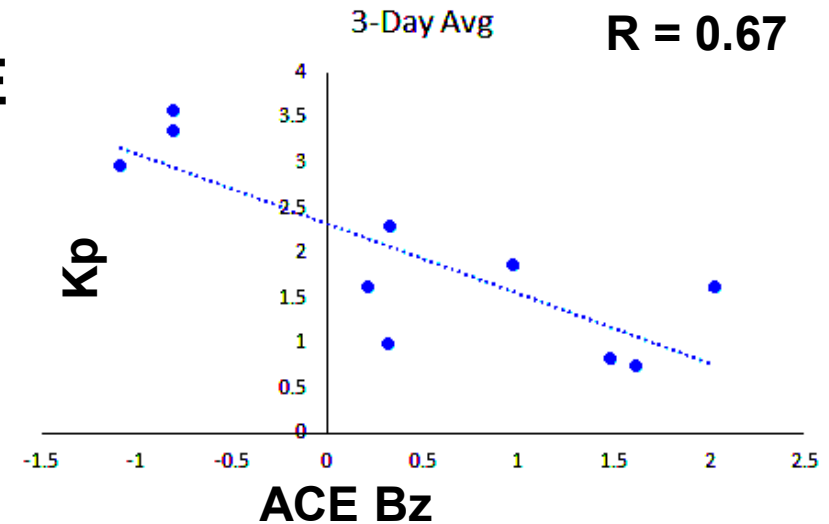
Different Techniques for Measurement of Bz

UCSD Prediction Analyses - 2016 Study

Dst vs GSM Bz (CR 2083) Kp vs GSM Bz



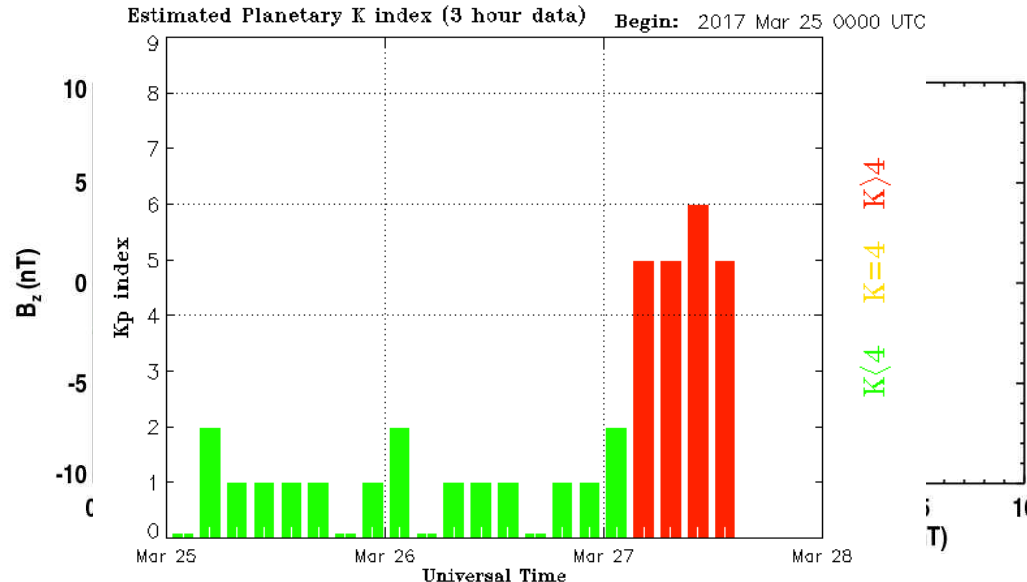
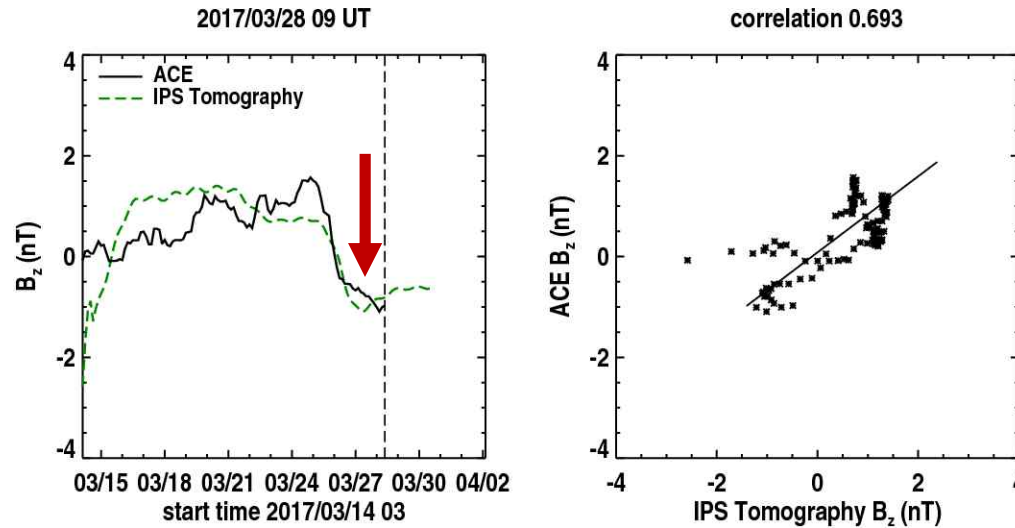
ACE



Different Techniques for Measurement of Bz

“Can’t possibly be right” - a good NOAA colleague

GSM Bz



**Largest min
-Bz**

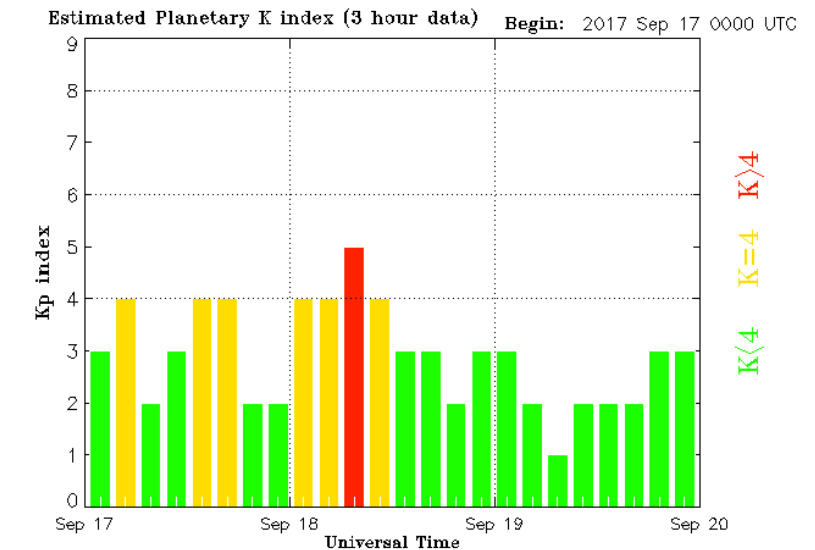
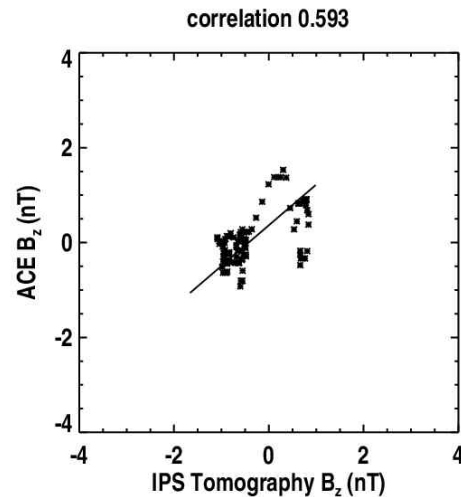
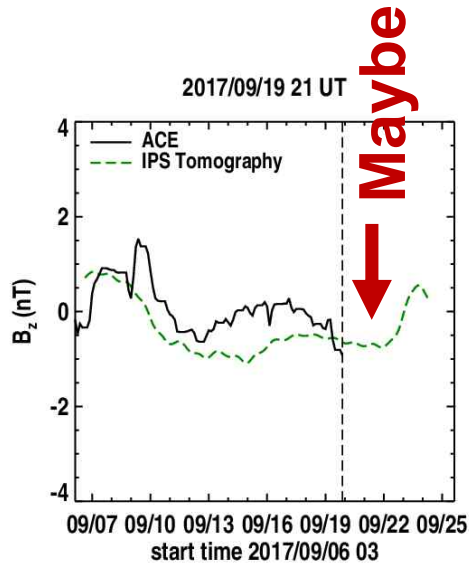
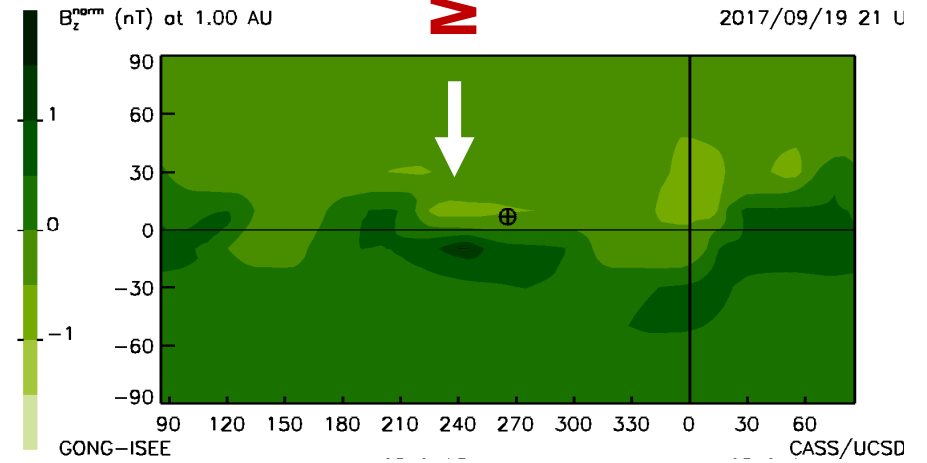
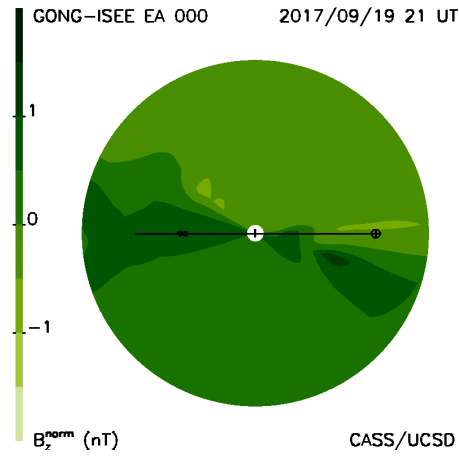
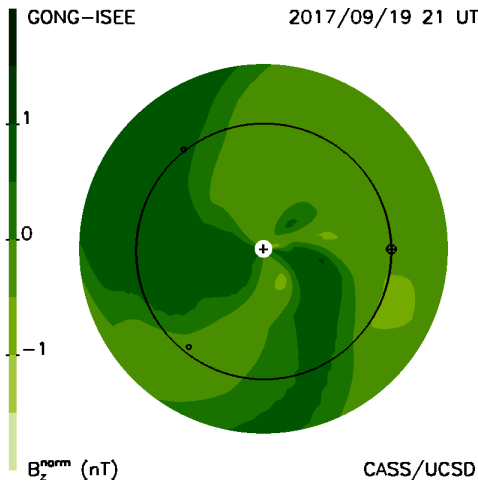
**-17nT 09 UT
03/27**

(Perhaps)

Different Techniques for Measurement of Bz

GSM Bz UCSD current prediction

Maybe



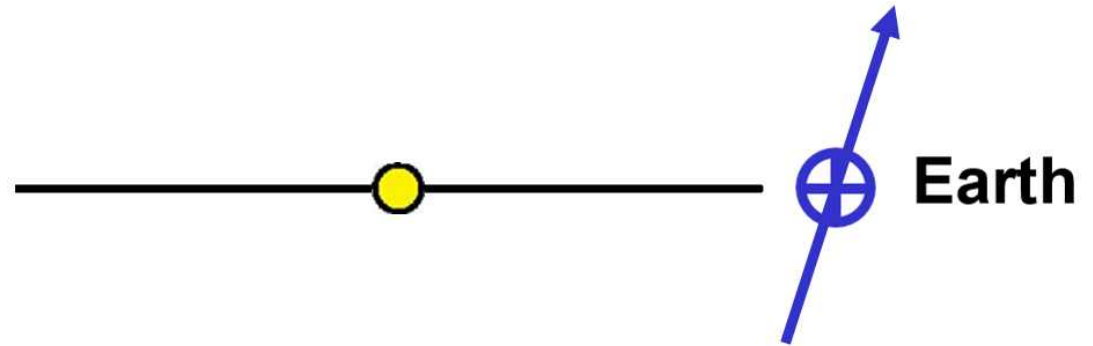
Updated 2017 Sep 20 00:30:03 UTC

NOAA/SWPC Boulder, CO USA

CASS/UCSD ISEST Bz 2017

Different Techniques for Measurement of Bz

Conclusions:



**Geocentric Solar
Magnetospheric (GSM) Bz:**

The reasons to determine Bz

**Concept studies: How we may be able to
determine Bz**

- 1) In CMEs.**
- 2) In the background solar wind**

Now there are some successes in determining Bz